nature portfolio

Peer Review File

Periodic confined cell migration drives partially reversible chromatin reorganization in cancer cell lines

Corresponding Author: Professor Maria Jose Gomez-Benito

This manuscript has been previously submitted at another journal. This document only contains information relating to versions considered at Communications Biology.

This file contains all reviewer reports in order by version, followed by all author rebuttals in order by version.

Version 0:

Reviewer comments:

Reviewer #1

(Remarks to the Author)
Article: Periodic confined cell migration drives partially reversible chromatin reorganization

Summary of the work:
The manuscript by del Valle Blazquez-Romero et al. investigates the reversibility of chromatin reorganization upon the transient exposure of cells to physically constrictive environments. They have created a custom-designed microfluidic device aimed to mimic the conditions of cell migration throughout tissues, and used it to perform single-cell analysis of chromatin dynamics during passage through alternate regions of confined and non-confined regions. The data addresses this question from two perspectives: nuclear area and volume, and the spatial organization of condensed chromatin regions within the nucleus. Regarding nuclear size, the authors report a reduction in both area and volume within constricted regions, followed by a recovery to pre-confinement levels once cells exit into unconfined areas. They also observe a general increase in nuclear size as cells progress along the channel. From the chromatin organization perspective, the proportion of condensed chromatin is reported to increase as cells pass through confined spaces. Although the ratio of condensed to uncondensed chromatin returns to baseline after release from confinement, the spatial distribution changes: condensed regions tend to form larger domains. The authors propose that confinement brings condensed regions into close proximity, promoting their coalescence through attractive interactions that persist even after de-confinement.

We recommend the following points be considered to strengthen the article's message and conclusions:

Comments/Questions:
In Figure 2:
1. It appears that imaging was performed in 2D, capturing only a single optical slice of the nucleus. Have you considered whether the observed changes in chromatin condensation ratio could be influenced by nuclear deformation during confinement, potentially bringing previously out-of-plane chromatin into the focal plane? How did you rule out this possibility?
2. Regarding the highly condensed areas: there is no mention of the intensity threshold between condensed and non-condensed area.
3. In figures 2b and 2f, have the authors accounted for the effect of nuclear shrinking under confinement on their measurements? Specifically, could the observed differences in the distribution of condensed chromatin sizes or intensities be partly driven by the reduced number of pixels in smaller nuclei, rather than biological reorganization? How is this disentangled in the analysis?
Figure 3:
4. In figure 3.b, we recommend significance annotations to be presented for every pair of neighboring groups of points. Similarly, a significance annotation regarding the normalized condensed area between different non-condensed states (N1, N2 etc.) would provide more clarity with respect to the reversibility of the nuclear condensation upon escape from confinement.
Figure 4:
5. In figure 4.b it would be good if a quantitative measurement of the difference in distributions can be provided. Think of

Wasserstein distances or Kolmogorov–Smirnov Test, as they should work with non-normal distributions such as here.
In figure 5:
6. In figure 5, it would be interesting to see a time-dependent evolution of the heterochromatin content of the cells as they progress through the device. For example, before any confinement, after a specific number of confinements, and after having crossed the whole distance of the channel. Does the heterochromatin ratio evolve?
7. In figure 5, section b there is an error bar suggesting that the analysis was done on multiple cells, but the N is not given. If the analysis was performed only on the cells displayed in the figure, it is strongly recommended to add more cells to the analysis. In this same figure the lower significance bar lacks its annotation.
Figure 6:
8. The simulation model is based on the assumption that regions of chromatin condensation undergo attractive forces to each other. However, no reference is provided to support this hypothesis.
9. In the simulation model, why was a harmonic spring used, when entropic springs with diverging cost at critical length could be a more reasonable choice in the context of chromatin?
10. In supplementary figure 4, a visualization of the equation (2) with these specific cutoffs is recommended.
11. The different axes for graphs c,d and e should be re-done; c and e are in minutes, whilst d is in seconds. Also, when converted in seconds, the timepoints from figure e correspond to none of the instances presented in graph d. Please provide more clarity here.
12. At what rate does the shape of the modelled nucleus change? Some timepoints are being displayed in Figure 6d: are there intermediate states between these, or do the nuclei “jump” from one displayed shape to the next?
Minor comments:
1. Page 3, line 5: The use of the term ‘instead’ here is not ideal. Something like ‘On the contrary’ or ‘Conversely’ would be more appropriate for the intended message.
2. In Page 3, line 8, the phrase “Mechanical forces shape chromatin architecture, resulting in histone modifications that influence gene expression and cell fate.” Implies a deterministic cause-effect relationship between chromatin architecture changes and histone modifications. Or, a direct and unidirectional path between the two is not supported by evidence. A more appropriate phrase would be: "Mechanical forces alter chromatin architecture, which can enable or modulate histone modifications…".
3. In page 4, at the end of paragraph 2, a reference could be useful in justifying how these specific dimensions reflect physiological constrictions.
4. Regarding the graphs 2b and 2f: the distribution of pixel intensity in cells during migration is addressed in the paper’s text after the measurements regarding the area (figures 2c and 2g). It would thus improve readability if the positions of these were switched in the figure (area plots above the intensity profiles).

Reviewer #2

(Remarks to the Author)
I co-reviewed this manuscript with one of the reviewers who provided the listed reports. This is part of the Communications Biology initiative to facilitate training in peer review and to provide appropriate recognition for Early Career Researchers who co-review manuscripts.

Reviewer #3

(Remarks to the Author)
In this study, we developed a microfluidic platform composed of alternating confining and non-confining regions, enabling real-time monitoring of chromatin dynamics in individual cells. Our results reveal that nuclear deformation within confined regions leads to a reversible increase in chromatin condensation. Notably, following deformation, condensed chromatin clusters adopt a distinct spatial organization, suggesting incomplete relaxation and thus only partially reversible condensation. Numerical simulations indicate that the interplay between nuclear deformation and attractive interactions among heterochromatin domains may underlie the observed chromatin reorganization. Based on the colledted results, the authors suggest that partially-reversible chromatin condensation acts as an adaptive mechanism in cancer cells to mediate both, gene expression regulation and persistent mechanical memory, which reveals the inherent duality in chromatin dynamics. The study presents compelling results; however, it would benefit from the inclusion of additional, currently missing information and clarification.

1. Did you notice corrlation between nucleus shape (e.g. circularity, aspect ratio, solidity) and condansation rate after each confinement? It would be worth to include such data.
2. “Our analysis revealed that the nucleus area exhibits a sudden drop when entering the confinement for every cell, regardless of their migration speed.” Coul you provide a correlation graph and calculation to obsreve the average speed of a cell and normalized nuclei area/condensation area to observe potential differences?
3. In the brightfield images of cells migrating through constrictions did you notice that cells migrating facter have a distinc morphological features (e.g. ameboidor elongated cell body)?
4. Cells traveled longer distances trought short channels than in long channels as depicted in the Figure 3 and Supplementary Material Sec. S3. Could you speculate why was it happening, was it associated with e.g. higher nuclear envelope rupture or DNA damage?
5. In Bastianello et al., 2024 (PMID: 38990945), in both utilized cell lines U2OS and HeLa, the speed of migration across constrictions increased linearly with the nuclear size, suggesting a direct relationship between cell cycle, size, and speed.

Did authors observe such correlation? Furthemore, in Bastianello et al., 2024 (PMID: 38990945) the authors observed that migration across constrictions can significantly delay cell cycle progression, was it also seen in this manuscript, what was division rate in the cell lines that you analyzed? Were there any differences between short and long channels?
6. As it was published that confined migration increases H3K9me3 and H3K27me3 heterochromatin marks that could persist for long time (Chieh et al., 2022, PMID: 36117991), the authors observed correlation between facultative heterochromatin loci (H3K27me 3 marker), which have been shown to increase more than constitutive heterochromatin (H3K9me 3 marker) upon confined migration. Was the total area of both markers H3K9me3 and H3K27me3 (both separate and merged) increased during passage through the constriction and after? Please perform such analysis.
7. In Figure 5b authors present a bar chart representing the spatial correlation coeffcient for chromatin distribution (green) against each heterochromatin marker (magenta and cyan), classified according to the confined state of the cell: confined or non-confined. It is not clear for me how the bar chart was genererated. Was it based on the images from Fig. 5a or a population of cells (which would be preferential). Which correlation coefficient was used (e.g. Pearson's)? Please provide also a scatter plots to visualize the correlation.
8. It is known that some proteins can accumulate in the front of cell's nucleus during confined migration, e.g. Nesprin-2 (PMID: 32419336, PMID: 40340251), potentially thethering heterochromating towards them. Did you observe increased heterochromatin markers towards the front of the nucleus when compared to the rear?
9. Confined migration can lead to increase nuclear envelope rupture events (PMID: 27013428). What was the nuclear envelope rupture rate in the conditions? Did you see any correlations between the chromatin condensation and NE rupture rate? How about the NE rupture rate after multiple passages?

Reviewer #4

(Remarks to the Author)
This well-written manuscript uses H2B-GFP–expressing cells and a microfluidic device to investigate chromatin dynamics during and after confined migration. The authors show that chromatin compacts as the nucleus transits through confinement and partially recovers after exit, but does not fully return to the pre-migration state. Notably, the distribution of condensed chromatin region sizes broadens following confinement, suggesting lasting changes in chromatin organization. Coarse-grained polymer simulations, excluding biochemical factors, further demonstrate that the observed behavior can be explained by purely physical chromatin reorganization. This work is timely, given the increasing interest in how confinement affects nuclear structure and function.
However, several major concerns need to be addressed before considering this manuscript for publication:
Major Points
• Sample size in Figure 2: Results are currently based on two cells (one slow and one fast migrating). Data from additional cells are necessary to establish reproducibility, particularly since this figure underpins the claim that confinement increases chromatin condensation range ("dispersion in pixel proportion towards opposing ends").
• Nuclear size correlation: In Figure 2, migration speed appears correlated with nuclear size. This relationship should be discussed, and subsequent analyses (Figure 3-5) should stratify cells by migration speed and nuclear size. Analysis of condensed area vs. nuclear area dynamics during confinement would be especially informative.
• Cell cycle state: Chromatin compaction and nuclear size are cell-cycle dependent. The authors should consider DNA replication block (e.g., thymidine treatment) to control for this.
• Clarification of "dispersion in pixel proportion": More explanation is needed. The intensity range seems stable, while the peak broadens, implying that the pixel intensity gets distributed within a constant range. Is this interpretation correct? The current description seems to imply that the intensity range (intensity min/max) increase with confinement.
• Image analysis transparency: The methods mention MATLAB processing, but the actual code and detailed description of the algorithm (e.g., which adaptive filter was used) should be included. This would enhance reproducibility and serve as a resource for the community.
• "Spatial distribution" terminology: Section 2.5 and other areas use this phrase, but quantification appears limited to size distribution. Size distribution does not reflect spatial distribution; please clarify.
• Sample size reporting: Numbers of analyzed nuclei are missing for Figures 4B–C and 5B. Please include sample sizes, define error bars (SD vs. SEM), and provide correlation coefficients for Figures 5E and 5H (as a representative value against the bar plot in 5B).
• Cluster number dynamics: The manuscript states that confinement brings heterochromatin regions closer, leading to persistent interactions. If true, the number of condensed regions should decrease during migration. Please quantify cluster number dynamics, which would also support the discussion statement that "small clusters disappear to form larger clusters."
Minor Points
• "We identified two distinct behavioral patterns, one associated with slow cells and the other with fast cells. The former comprises cells that traverse the confinement in less than 40 minutes, whereas the latter includes cells requiring a longer time to complete the traversal." -- The sentence describing migration speed patterns is flipped—fast vs. slow cells are mislabeled.
• All microscopy images should include scale bars.
• In Figure 2, panels B and F are referenced later in the text; consider repositioning them. Their legend should also explain the red bar (presumably confinement). Panel H is missing its label.
• Fig. 3B and C, what are the data normalized to? Why the data is not 1 at entry? Consequently, what is "one" referring to in the following sentence: "Furthermore, we noted that the mean for every non-confining region is approximately one, …"
• In Figure 4B, annotate Acon and Atot in the legend.
• The description on H3K27me3 and H3K9me3 from the Method section should be included in the Results section. This will provide context to the reader on why these markers are chosen to begin with.
• "It is noteworthy that H3K9me3 marker (magenta channel) is preferentially expressed in the nuclear periphery and around

the nucleolus (Figure 5) …" – Isn't the H3K27me3 also enriched at the nuclear periphery and around the nucleolus?
• In Figure 5, H3K9me3 and H3K27me3 are immunostained, not GFP fusions; the "GFP" label should be removed.
• Figure 5B should be presented later in the figure, as it is the conclusive data from the images.
• "The recovery is not complete, since the peak in chromatin density shifts to smaller values compared to nuclei before the confinement (Figure 6c)." – this is not clear, which part of the data show this observation?
• Figure 6E is very hard to follow. The text refers the figure in seconds while the data is in minutes. Please consider changing the color scheme as it is very hard to distinguish the early time points. Arrows with different colors (with description in the figure legend) might help in describing the statement in the text: "The widening in chromatin distribution during confinement is appreciated by comparing the histograms for t = 270 s and t = 541 s. The height of the peak decreases, and the tail of the distribution rises. After confinement, corresponding to t = 1081 s and t = 1622 s, density distribution is partially recovered (⇢ = 0.2). The values of the density distribution for ⇢ > 0.2 are higher than for the unconstricted nucleus, suggesting a certain degree of irreversible behavior after confinement."
• "We find that the distribution for small chromatin cluster sizes is not characterized by a power-law distribution as in the case of nucleoli [43, 44] but by an exponential distribution, similar to that observed for intracellular protein condensates [42]." – please provide more explanation on this statement.
• "However, we consistently find probability peaks at higher cluster areas during confinement, which are absent in the case of protein condensates or nuclear speckles [42]." – what "probability peaks at higher cluster areas" means, how it correlate with Reference [42], and what is the impact of this comparison?
• Product codes for antibodies are missing and should be provided.

Version 1:

Reviewer comments:

Reviewer #1

(Remarks to the Author)
Paper review: Periodic confined cell migration drives partially reversible chromatin reorganization
- Joint report for evaluation of reviews –

Shivashankar GV, Leonard Piroska
We have reviewed the new version of the manuscript "Periodic confined cell migration drives partially reversible chromatin reorganization". We believe that our suggestions and concerns have been addressed in this new version. Please find below a more detailed report comprising our main questions, and a summary of how these were answered by the authors.

1. It appears that imaging was performed in 2D, capturing only a single optical slice of the nucleus. Have you considered whether the observed changes in chromatin condensation ratio could be influenced by nuclear deformation during confinement, potentially bringing previously out-of-plane chromatin into the focal plane? How did you rule out this possibility?
To address this, the authors provided a finite element simulation of the theoretical vertical displacement within the constricted nuclei. The model shows vertical displacements on the order of 20–120 nm, far below the axial resolution of typical fluorescence imaging, supporting the idea that chromatin movement is predominantly in the x–y plane under strong vertical confinement. It is true that, as with any simplified FEM, this does not fully exclude potential biological sources of z-motion (e.g., cytoskeletal forces, nuclear rocking). Still, the very low simulated z-displacements make it unlikely that vertical forces appreciably influence chromatin condensation. The authors acknowledge the experimental limitation of the 2D imaging in the new version.

2. Regarding the highly condensed areas: there is no mention of the intensity threshold between the condensed and non-condensed areas.
The authors provided more details with respect to the analysis methods used for segmenting highly condensed chromatin areas. The pixels below 0.6 (normalized between 0 and 1) are not considered. For those above 0.6, a threshold based on local intensity distribution is used. This has been used before, it allows to account for potential problems related to illumination uniformity and contrast changes, which can occur when the geometry of the cell is perturbed by the constriction. The choice is approved.

3. In figures 2b and 2f, have the authors accounted for the effect of nuclear shrinking under confinement on their measurements? Specifically, could the observed differences in the distribution of condensed chromatin sizes or intensities be partly driven by the reduced number of pixels in smaller nuclei, rather than biological reorganization? How is this disentangled in the analysis?
They take into account these area effects, and provide a new graph, which shows the evolution of basal condensed chromatin content divided by the instantaneous nuclear area. This yields the expected fraction of the nucleus that would be condensed if the condensed area did not change at all and only the nucleus area changed.

4. In figure 3.b, we recommend significance annotations to be presented for every pair of neighboring groups of points. Similarly, a significance annotation regarding the normalized condensed area between different non-condensed states (N1, N2 etc.) would provide more clarity with respect to reversibility of nuclear condensation upon escape from confinement.
They provided an excel file with the significance annotations in Supplementary Materials

5. In figure 4.b it would be good if a quantitative measurement of the difference in distributions can be provided. Think of

Wasserstein distances or Kolmogorov–Smirnov Test, as they should work with non-normal distributions such as here.
They provided a graph with the Wasserstein distances.

6. In figure 5, it would be interesting to see a time-dependent evolution of the heterochromatin content of the cells as they progress through the device. For example, before any confinement, after a specific number of confinements, and after having crossed the whole distance of the channel. Does the heterochromatin ratio evolve?
The authors raise concerns about experimental limitations of doing immunofluorescence in the compression channel, which limit the feasibility of the suggested experiment.

7. In figure 5, section b there is an error bar suggesting that the analysis was done on multiple cells, but the N is not given. If the analysis was performed only on the cells displayed in the figure, it is strongly recommended to add more cells to the analysis. In this same figure the lower significance bar lacks its annotation.
All good, they added the N.

8. The simulation model is based on the assumption that regions of chromatin condensation undergo attractive forces to each other. However, no reference is provided to support this hypothesis.
They have provided references.

9. In the simulation model, why was a harmonic spring used, when entropic springs with diverging cost at critical length could be a more reasonable choice in the context of chromatin?
They provide several references indicating that using a harmonic spring in polymer models of chromatin is widely used.

10. In supplementary figure 4, a visualization of the equation (2) with these specific cutoffs is recommended.
They have added a graph.

The rest of the points are minor remarks related to phrasing, references and graph layouts, which the authors have addressed.

Reviewer #2

(Remarks to the Author)
I co-reviewed this manuscript with one of the reviewers who provided the listed reports. This is part of the Communications Biology initiative to facilitate training in peer review and to provide appropriate recognition for Early Career Researchers who co-review manuscripts.

Reviewer #3

(Remarks to the Author)
I would like to thank authors for the careful evaluation of their manuscript. All comments and suggestions raised by the reviewers have now been thoroughly addressed and incorporated into the revised version of the manuscript. I believe that these revisions have significantly improved both the clarity and the quality of the work. I kindly encourage consideration of the revised manuscript for publication in the journal.

Reviewer #4

(Remarks to the Author)
The authors have addressed all of the comments adequately.

Reply to Reviewer #1

Summary of the work:

The manuscript by del Valle Blazquez-Romero et al. investigates the reversibility of chromatin reorganization upon the transient exposure of cells to physically constrictive environments. They have created a custom-designed microfluidic device aimed to mimic the conditions of cell migration throughout tissues, and used it to perform single-cell analysis of chromatin dynamics during passage through alternate regions of confined and non-confined regions. The data addresses this question from two perspectives: nuclear area and volume, and the spatial organization of condensed chromatin regions within the nucleus. Regarding nuclear size, the authors report a reduction in both area and volume within constricted regions, followed by a recovery to pre-confinement levels once cells exit into unconfined areas. They also observe a general increase in nuclear size as cells progress along the channel. From the chromatin organization perspective, the proportion of condensed chromatin is reported to increase as cells pass through confined spaces. Although the ratio of condensed to uncondensed chromatin returns to baseline after release from confinement, the spatial distribution changes: condensed regions tend to form larger domains. The authors propose that confinement brings condensed regions into close proximity, promoting their coalescence through attractive interactions that persist even after de-confinement.

We recommend the following points be considered to strengthen the article's message and conclusions.

Reply: We would like to thank the reviewer for their time and insightful comments, which have helped to improve the quality of our manuscript. Below, we provide detailed responses to each specific issue raised by the reviewer. All changes made to address the comments from Reviewer #1 are highlighted in red in the revised manuscript.

Comments/Questions:

1. It appears that imaging was performed in 2D, capturing only a single optical slice of the nucleus. Have you considered whether the observed changes in chromatin condensation ratio could be influenced by nuclear deformation during confinement, potentially bringing previously out-of-plane chromatin into the focal plane? How did you rule out this possibility?

Reply: Thank you for raising this concern. Our imaging acquisition captures indeed a single 2D slice centered on the middle of the microchannels. Performing single-cell 3D imaging posed an increased risk of phototoxicity-induced cell death, which ultimately required us to lower the frame rate. Therefore, to prioritize temporal resolution (one frame every 10 minutes throughout 24-hour migration), we carefully considered the limitations of 2D imaging when designing our microchannels.

To prevent significant chromatin shifts along the vertical direction, our microchannels are engineered with a constant height of 6 µm in order to vertically confine the cells throughout the experiment (see Figure R1a). As a result of vertical confinement, cells exhibit a pseudo-2D deformation state, characterized by predominant deformation in the transverse plane (x-y plane). We were not able to experimentally rule out the possibility of chromatin movement along the vertical direction; however, we performed a simple finite element simulation to demonstrate numerically that movement within the nucleus is restricted to the transverse plane during our deformation under vertical confinement (Figure R1b).

We agree with the reviewer that this issue was overlooked in the original manuscript, and the following paragraph was included in Results section 2.1 when describing the confining geometry:

"As a result of vertical confinement, cells exhibit a pseudo-2D deformation state, characterized by predominant deformation in the transverse plane (x-y plane, see Figure 1). The nature of this deformation suggests that chromatin movements in the vertical direction are unlikely to be influenced by the confinement. Consequently, these vertical fluctuations can be considered negligible, which supports our 2D imaging strategy. Focusing on a single optical slice of the nucleus minimizes cell phototoxicity and allows for shorter time-lapse intervals which ultimately improves temporal resolution."

We incorporated the statement below in the discussion to acknowledge this issue as a limitation:

"While our study provides compelling evidence that nuclear deformation under confinement is accompanied by adaptive chromatin rearrangements, further investigation is needed to elucidate how the deformation influences chromatin plasticity and its role in long-term epigenetic changes. To prioritize high temporal resolution while minimizing cell phototoxicity, we opted for a 2D imaging approach. This trade-off allowed for higher frame rates but limits a full three-dimensional characterization, which could be addressed in future studies with volumetric imaging."

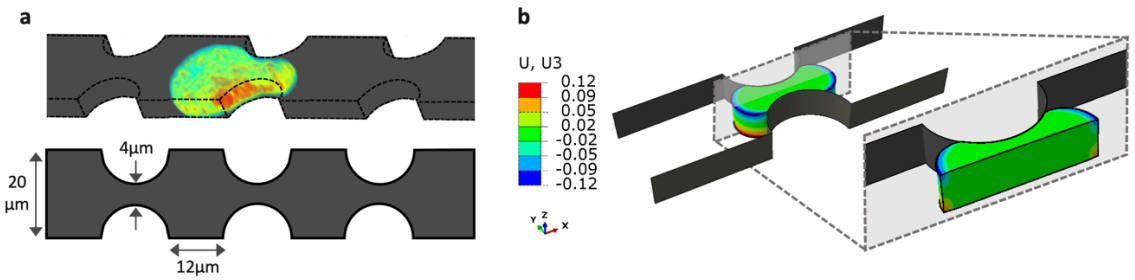

Fig. R1. a Three-dimensional reconstruction of the confining microchannel containing confocal imaging of a PACA-H2B-GFP cell migration through a constriction. Note the constant height between confining and non-confining regions. **b** Finite element simulation representing the displacement in the vertical direction (U3 in µm) for the constricted nucleus.

2. Regarding the highly condensed areas: there is no mention of the intensity threshold between condensed and non-condensed area.

Reply: Thank you for pointing this out. We agree that the segmentation for highly condensed areas should be more thoroughly described in our manuscript. Our algorithm to identify these chromatin clusters relies on an adaptive filter which selects a specific threshold according to local mean intensity in neighboring pixels. Furthermore, pixels with intensities lower than 0.6 (normalized between 0 and 1) were excluded from the analysis regardless of the local threshold. Similar segmentation algorithms using this MATLAB function have already been used in the literature [57-59]. To address the reviewer's comment, we modified the Methods section 4.6:

"Finally, a custom MATLAB script implementing an adaptive image filter was used to compute the binary mask that identifies highly-condensed chromatin regions. This algorithm excludes pixels with intensities lower than 0.6 (normalized intensity) and it relies on the MATLAB function *adaptthresh* to select specific thresholds for the segmentation according to local mean intensity in neighboring pixels. Similar segmentation algorithms using this MATLAB function have already been described in the literature [59-61]. The evolution of these chromatin clusters over time is then addressed through histograms representing their relative area within the nucleus for every region in the microchannel."

[59] Karrobi, K. et al. Fluorescence lifetime imaging microscopy (flim) reveals spatial-metabolic changes in 3d breast cancer spheroids. *Scientific Reports* **13**, 3624 (2023).

[60] Heinrich, S. et al. Glucose stress causes mrna retention in nuclear nab2 condensates. *Cell Reports* **43**, 113593 (2024).

[61] Zonca, L. et al. Unveiling the functional connectivity of astrocytic networks with astronet, a graph reconstruction algorithm coupled to image processing. *Communications Biology* **8**, 114 (2025)

3. In figures 2b and 2f, have the authors accounted for the effect of nuclear shrinking under confinement on their measurements? Specifically, could the observed differences in the distribution of condensed chromatin sizes or intensities be partly driven by the reduced number of pixels in smaller nuclei, rather than biological reorganization? How is this disentangled in the analysis?

Reply: We appreciate the reviewer's insightful comment and agree that clarifying this aspect strengthens the manuscript. We did consider nuclear shrinking when interpreting our chromatin condensation results. Our analysis indicates that nuclear shrinking is minimal—typically limited to a reduction of 15–20 μm² in large nuclei—and thus it cannot account for the measured two- to three-fold increases in basal chromatin condensation. To further support this conclusion, we have included a plot (gray curve in Figure R2b) displaying basal condensed chromatin content as a function of nuclear area for each frame:

$$y(t) = \frac{\bar{A}_{\mathrm{cond}}(t_{NC})}{A_{\mathrm{nucleus}}(t)}$$

where $\bar{A}_{\mathrm{cond}}$ is the average condensed chromatin area among the frames in which the cell is unconfined (t_{NC}), i.e. during all non-confining regions Entry, N1, N2…, and $A_{\mathrm{nucleus}}(t)$ is the nuclear area in frame t.

Then, $y(t)$ represents the changes in condensed chromatin area attributed exclusively to changes in nuclear size (gray curve in Figure R2b). The curve exhibits a subtle increase upon confinement due to nuclear shrinking; however, this limited growth does not explain our peaks in chromatin condensation in the purple curve.

Regarding spatial resolution, while there is room for improvement, our imaging approach still captures biological reorganization at the single-cell level. For example, the smallest nucleus analyzed had an area of 22.46 µm², corresponding to 4,319 pixels. Therefore, the resolution is sufficient to attribute differences in intensity and cluster size to genuine biological effects, rather than technical limitations.

To address this comment in our original manuscript, we modified Figure 2d,h to include the contribution of nuclear shrinking in the quantification of chromatin condensation (gray curve) and we added the following statement in Results Section 2.2:

"This trend for highly-condensed chromatin regions suggests that, upon cell deformation during confined migration, chromatin condensation level increases reversibly. After deformation, the nucleus recovers its basal chromatin condensation state which generally lies around 5 to 10% of the total nucleus area. Note that the twofold to threefold increase in highly-condensed chromatin area cannot be explained by the decrease in nuclear area upon confinement. To represent the contribution of nuclear shrinking in the quantification of chromatin condensation, the gray line in Figure 2c,g displays basal condensed chromatin content divided by the instantaneous area of the nucleus. Basal condensed chromatin represents the mean highly-condensed chromatin area of the nucleus averaged over all non-confining regions (Entry, N1, N2…). Then, its evolution along the microchannel (gray curve) illustrates the changes in chromatin condensation induced by changes in nuclear area only. The notably limited growths during confinement do not to explain the peaks in the segmentation of condensed chromatin area (in purple in Figure 2c,g)."

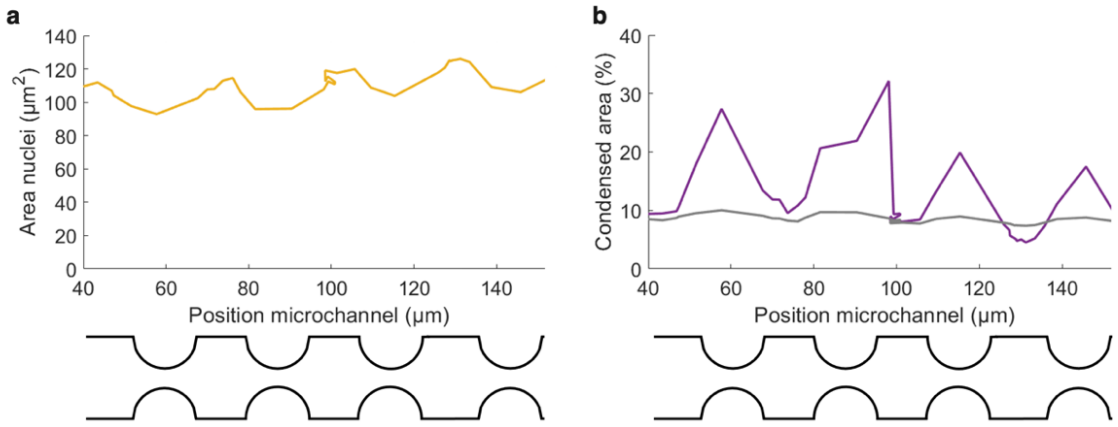

Fig. R2. a Evolution of the nucleus area for a representative A549-H2B-GFP cell migrating fast through short confining microchannels. **b** For the same cell, evolution of the relative highly-condensed chromatin area representing the percentage of the nucleus segmented as condensed chromatin (purple) and the evolution of basal condensed chromatin content divided by the instantaneous nuclear area (gray). The latter displays the changes in chromatin condensation induced exclusively by changes in nuclear size. The notably limited increases in gray during confinement do not explain the peaks in chromatin condensation in purple.

4. In figure 3.b, we recommend significance annotations to be presented for every pair of neighboring groups of points. Similarly, a significance annotation regarding the normalized condensed area between different non-condensed states (N1, N2 etc.) would provide more clarity with respect to reversibility of nuclear condensation upon escape from confinement.

Reply: We appreciate your suggestion and have revised the figure accordingly. Due to the limited space in the graph and for the sake of clarity, we are including a spreadsheet containing the

significance annotations for every pair of groups in the Supplementary Material. The caption of the figure has been modified to include a reference to the table:

"See Supplementary Spreadsheet S1 for the significance results among every pair of groups."

Additionally, Supplementary Spreadsheet S1 has also been referenced when comparing non-condensed states to establish a baseline level for chromatin condensation in section 2.4:

"In addition, our population-level results also reflect the growing trend in nuclear area that was identified during the single-cell analysis; note the statistically significant difference between the mean for the normalized nucleus area in the entry and in N4 (see Supplementary Spreadsheet S1 for the p-value between these two groups). A lower number of cells reach the end of the microchannels, hence, the last regions adjacent to C5 are not considered statistically significant owing to the reduced number of data points.

The results for the normalized relative area of highly-condensed chromatin regions reveal that the mean for chromatin condensation level during every confining region is significantly higher than the mean for adjacent non-confining regions (Figure 3b, right). Furthermore, we noted that the mean for non-confining regions is approximately one, i.e. a cell has a similar mean condensed area in every non-confining region (p-values between non-confining regions failed to meet the significance criterion, see Spreadsheet S1) . This supports the idea of a basal chromatin condensation level; nuclei stably recover their original condensation level after every constriction, proving the reversibility of global chromatin condensation in these confinement devices. "

5. In figure 4.b it would be good if a quantitative measurement of the difference in distributions can be provided. Think of Wasserstein distances or Kolmogorov–Smirnov Test, as they should work with non-normal distributions such as here.

Reply: Thank you for your comment. We agree that quantitatively assessing the differences between our distributions for chromatin cluster size could significantly improve our manuscript. The Kolmogorov-Smirnov Test is primarily intended for pairwise (two-sample) comparisons. Since our analysis involves multiple groups, we opted to follow your suggestion of applying Wasserstein distances. We implemented a code in MATLAB which uses the function from Niklas Kolbe [47] to compute Wasserstein distances in 1D distributions and then, displays a heatmap to represent the results for each pairwise comparison (Fig. R3a).

Your suggestion clearly improves the manuscript and, therefore, we decided to further apply this method to quantitatively assess the differences between the distributions for the number of chromatin clusters per cell (a new analysis suggested by another reviewer), see Figure R3b. Consequently, we included these heatmaps in the supplementary section (Fig. S7) with a brief description of the results in the caption and the following statement in the manuscript Section 2.5:

"This finding implies that, despite basal condensation levels are restored, the spatial distribution of highly-condensed chromatin regions within the nucleus is not fully recovered after chromatin reorganization upon nuclear deformation. To quantify how different the distributions are one to another, we computed the Wasserstein distances [48] (Supplementary Figure S7a, left). This pairwise comparison leads to notably shorter distances when comparing regions of the same confining category, either confining or non-confining. Distributions for the same confinement state are more similar among each other and, hence, these results align with reversible chromatin condensation. However, it is noteworthy that the distance between the Entry and the remaining non-confining regions increases with the number of confinements traversed by the cells. Interestingly, when pairing a confining region with a non-confining one, the Wasserstein distance consistently decreases as the

non-confining region is located further downstream in the microchannel. This implies that, as the cell overcomes more confinements, the distribution of chromatin cluster sizes in non-confining regions aligns more closely with those in confining regions. This trend supports our conclusion that cluster size distribution shifts towards larger values, characteristic of distributions during confinement, as the cancer cell migrates through successive confinements.

…

This explanation accounts for the simultaneous increase in cluster size and reduction in cluster number. Similarly to cluster size, the results for the pairwise comparison using Wasserstein distances (Supplementary Figure S7a, right) shows closer resemblance between distributions for regions of the same confining state and a trend towards shorter distance values when comparing confinements with non-confining regions further downstream the microchannel. Consequently, these results align with cluster size distributions to support that chromatin condensation during confined migration is only partially reversible for the 4x6µm^2 constrictions in our microfluidic devices."

We additionally explained how Wasserstein distances were calculated in Methods section 4.6:

"Subsequently, the differences among the distributions for each region were quantified using Wasserstein distances, which indicate how similar two probability distributions are such that smaller distance values correspond to more resembling distributions. This pairwise comparison was implemented in MATLAB based on the code published by Kolbe [48]."

[48] Kolbe, N. nklb/wasserstein-distance: v1.0. https://doi.org/10.5281/zenodo.10912241 (2024). Version v1.0

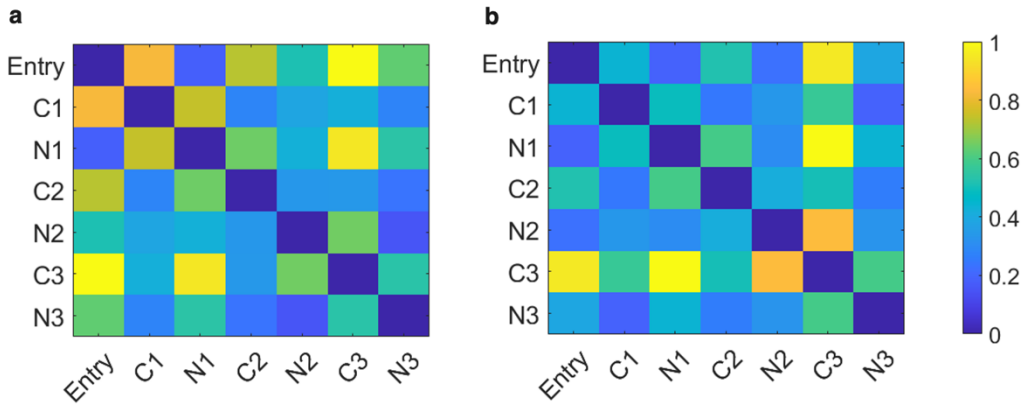

Fig. R3. Heatmap for the Wasserstein distances of the pairwise comparison of (**a**) chromatin cluster size and (**b**) number of clusters per cell distributions in each microchannel region. Wasserstein distances represent how similar two distributions are such that smaller distance values correspond to more resembling distributions. Wasserstein distances are normalized relative to the maximum value in each heatmap. Note that shorter distances support how similar the distributions are among confinements and among non-confining regions. Interestingly, the Wasserstein distance for every confinement paired with a non-confining region decreases notably as the non-confining region locates further downstream the microchannel in both, cluster size and cluster number analysis.

Figure 5:

6. In figure 5, it would be interesting to see a time-dependent evolution of the heterochromatin content of the cells as they progress through the device. For example, before any confinement, after a specific number of confinements, and after having crossed the whole distance of the channel. Does the heterochromatin ratio evolve?

Reply: We thank the reviewer for this interesting suggestion. We agree that performing a quantitative, time-dependent analysis of heterochromatin evolution would add significant value to our study. Nevertheless, our current experimental setup imposes practical constraints.

To identify heterochromatin loci within cell nuclei, we fixed the cells after 24 hours of migration and performed immunostaining using two well-established heterochromatin markers, H3K9me3 and H3K27me3. The confining microchannels, however, generate a complex diffusion gradient of the staining reagents, which results in nonuniform marker distribution when multiple cells occupy a single channel. As a result, suggesting a time-dependent evolution of chromatin requires accounting for diffusion-related variability and comparing cells located at different positions along the microchannel. To mitigate these diffusion effects, introducing a complementary euchromatin marker such as H3K9ac could be used to compute a heterochromatin-to-euchromatin ratio which is then normalized among cells. Nonetheless, our cell line expresses intrinsic nuclear GFP, which limits the availability of laser lines for additional fluorophores and prevents simultaneous imaging of H3K9me3, H3K27me3, and H3K9ac in a single sample.

To acknowledge this limitation, we included the following statement in the Discussion of the manuscript:

"Despite this improved time-lapse interval (one frame every 10 minutes), our temporal resolution is not sufficient to capture rapid enzyme-mediated heterochromatin dynamics. Another limitation of our study arises from intercellular variability during the heterochromatin loci analysis. To identify heterochromatin domains within cell nuclei, cells were stained for two well-established heterochromatin markers, H3K9me3 and H3K27me3. However, the confining microchannels used in our experiments generate complex diffusion gradients of the staining reagents, leading to nonuniform marker distribution when multiple cells occupy the same channel. This effect introduces additional variability that constraints the precision of quantitative comparisons across nuclei. To compensate for diffusion-related variability, future analyses could include a complementary euchromatin marker (e.g., H3K9ac) to normalize the staining by computing the heterochromatin-to-euchromatin ratio in each cell. Addressing this limitation in the future could be interesting to study the evolution of persistent heterochromatin marks as the cells migrate further in the microchannel [30]. Future studies should aim at single-cell sequencing to unravel how the deformation triggers specific chromatin states and epigenetic marks and should employ higher-resolution or real-time imaging techniques to capture finer-scale chromatin dynamics."

7. In figure 5, section b there is an error bar suggesting that the analysis was done on multiple cells, but the N is not given. If the analysis was performed only on the cells displayed in the figure, it is strongly recommended to add more cells to the analysis. In this same figure the lower significance bar lacks its annotation.

Reply: We completely agree with the reviewer and the pertinent changes have been incorporated to the figure. Specifically, the results displayed in Figure 5 were analyzed for 18 confined cells and 123 non-confined cells after 24h migration through the microfluidic device.

Figure 6:

8. The simulation model is based on the assumption that regions of chromatin condensation undergo attractive forces to each other. However, no reference is provided to support this hypothesis.

Reply: We would like to thank the reviewer for highlighting this oversight. Several chromatin simulation polymeric models use an attractive potential between representing heterochromatin and/or LAD beads. Besides the model from Safran's group, which we are using as reference for our specific model, we have added to the manuscript and to the supplementary material two other references.

[24] Adame-Arana, O., Bajpai, G., Lorber, D., Volk, T. & Safran, S. Regulation of chromatin microphase separation by binding of protein complexes, *eLife* 12:e82983 (2023).

[69] Câmara, A. S. & Mascher, M. Consistencies and contradictions in different polymer models of chromatin architecture. *Computational and Structural Biotechnology Journal*, **21**, 1084–1091 (2023).

We have added these references in the second to last paragraph before the acknowledgements:

"...this potential includes attractive interactions among heterochromatin beads and, optionally, between heterochromatin and the nuclear lamina [24, 64, 69] (see Figure 6)...".

9. In the simulation model, why was a harmonic spring used, when entropic springs with diverging cost at critical length could be a more reasonable choice in the context of chromatin?

Reply: We thank the reviewer for their comment, and we believe they refer to a FENE-like potential. Even though FENE-like potential is also a valid choice, many recent studies implementing polymer models for chromatin use harmonic potentials (see a list of references below). We define a very high elastic constant for the bond ($K=128k_BT$) in order to maintain an almost constant bond length with fluctuations smaller than 10%, specifically $\sqrt{1/128} \times I_0$. For these small deformations a FENE-like potential is very close to a harmonic potential.

We have added to the main text and the Supplementary Material a couple of references regarding the use of harmonic potential in polymer models of chromatin:

[66] Bajpai, G. & Safran, S. Mesoscale long-time mixing of chromosomes and its connection to polymer dynamics. *PLOS Computational Biology* **19**, 1–30 (2023)

[67] Amitai, A. & Holcman, D. Polymer physics of nuclear organization and function. Physics Reports **678**, 1–83 (2017)

G. Bajpai and S. Safran [66] show that the use of a FENE or a harmonic potential does not make any difference in the calculations of scaling properties of mixing dynamics of chromosomes. A. Amitai and D. Holcman [67] review recent polymer models of chromatin and the harmonic potential is the only one used.

The references have been incorporated at the beginning of the second paragraph of section 4.9:

"The simulation particles (each representing approximately 250 nucleosomes, which we will refer to as beads from now on) are linked by harmonic springs [66,67] (corresponding to chromatin fiber)...".

10. In supplementary figure 4, a visualization of the equation (2) with these specific cutoffs is recommended.

Reply: We appreciate your suggestion, and we have accordingly redrawn the figure to incorporate the potential profile given by equation (2) and the corresponding cutoffs (Fig. S4b):

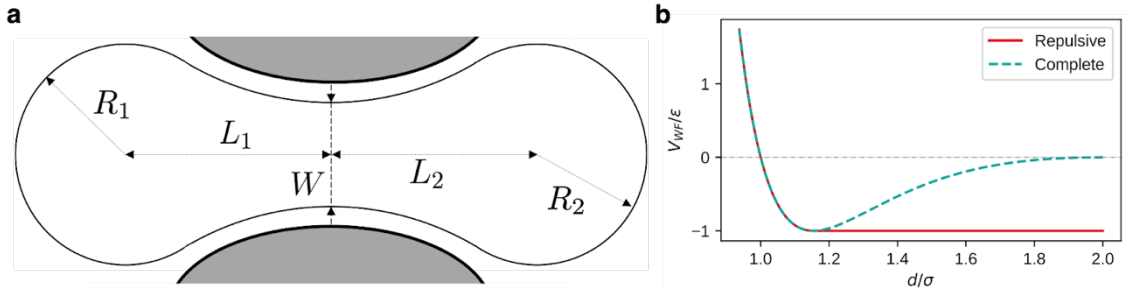

Supplementary Figure S9 a. Schematic of the geometry for the confined cell projected on the transverse plane. The indents defining the constriction in the channel are colored in gray. **b.** Graphical representation of the W–F potential described in equations (2) and (3). Both interaction types are displayed: the complete potential (green dashed outline) and the purely repulsive form (solid red line), truncated at $d/\sigma = 2/\sqrt{3}$.

11. The different axes for graphs c,d and e should be re-done; c and e are in minutes, whilst d is in seconds. Also, when converted in seconds, the timepoints from figure e correspond to none of the instances presented in graph d. Please provide more clarity here.

Reply: We thank the reviewer for pointing this out. We have unified the units in the graph to minutes. Note that the snapshot of Fig. 6d corresponds to the distribution profiles in Fig. 6e (since we rounded the time in seconds to minutes). We hope these changes provide clarity (see below Figure 6).

12. At what rate does the shape of the modelled nucleus change? Some timepoints are being displayed in Figure 6d: are there intermediate states between these, or do the nuclei "jump" from one displayed shape to the next?

Reply: Thank you for concern. In our model, the change in nucleus shape is defined in a continuous way. We have modified the Supplementary Material to explicitly state the rate of change of the distance L1 (0,4 microns/sec). The images in Figure. 6d are simple snapshots of the full deformation sequence. In fact, the complete sequence is shown in Supplementary Movie S2.

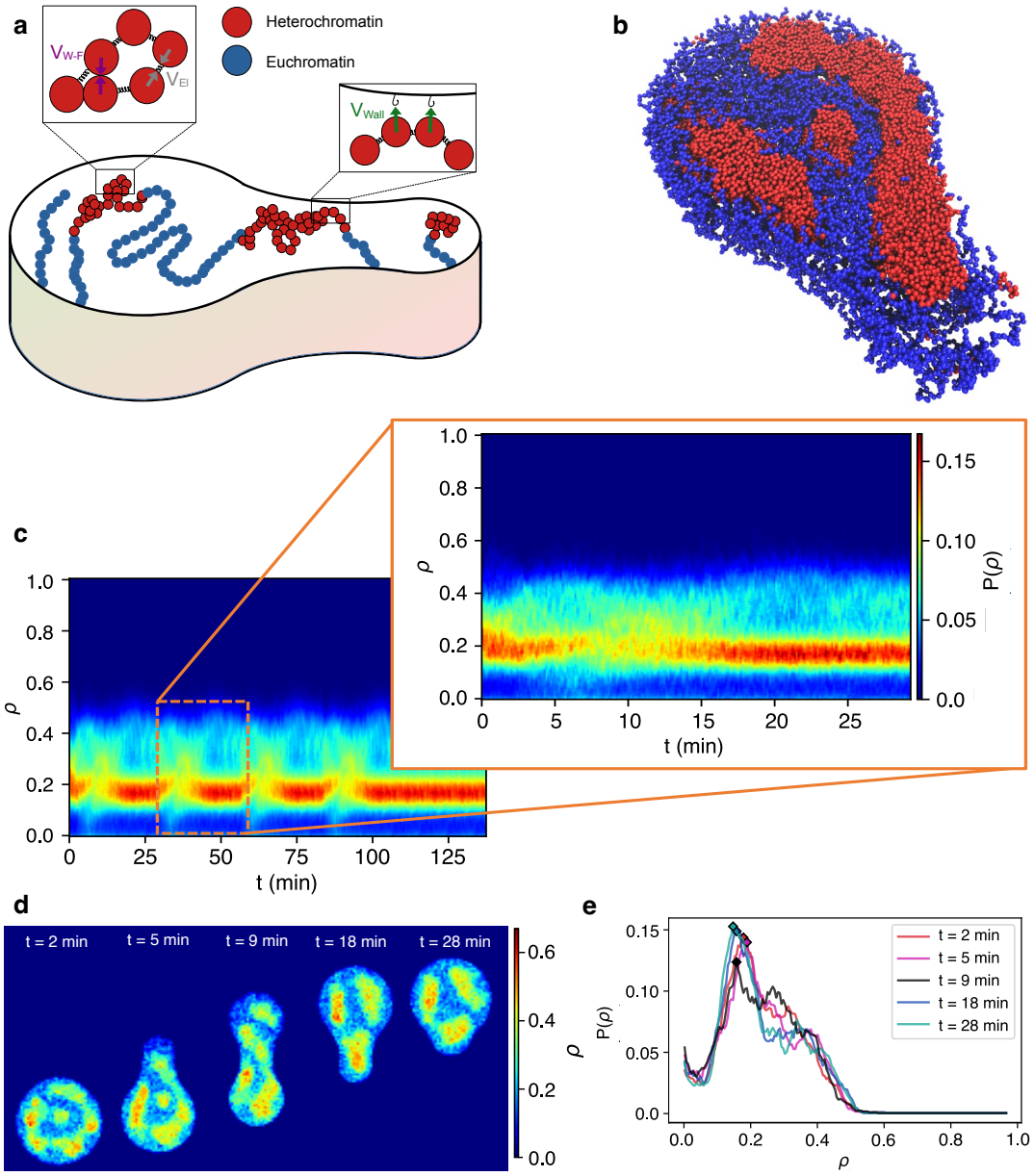

Fig. 6. Polymer model to simulate chromatin dynamics during cell migration through a confinement. a Schematic of the chromatin model showing heterochromatin (in red), euchromatin (in blue) and elastic (V_{El}), Wang-Frenkel (V_{W-F}) and Wall (V_{Wall}) potentials in the insets of the figure. The geometry corresponds to a cell nucleus traversing a constriction within the microchannel. **b** Three-dimensional polymer representation of chromatin (heterochromatin beads in red and euchromatin beads in blue) within the nucleus as it enters a constriction (t ≈ 5 min). The figure shows the bottom region of the nucleus, sectioned at the mid-width plane. **c** Colormap depicting the evolution over time (horizontal axis) of the histogram of chromatin density (vertical axis) for a chromatin chain of N=60000 and average domain size of 64 beads. The colormap corresponds to the pixel proportion with a particular density. The zoomed-in graph (right) represents chromatin density profile for the simulation performed (30 minutes long) while the complete graph (left) displays a repetition of the simulation result (i.e. the zoomed-in graph) to reproduce the experimental time-scale for successive confinements in fast migrating cells. **d** Chromatin density distribution within the nucleus as it dynamically deforms to replicate the migration through a constriction in the microchannel. The time corresponding to each snapshot is shown on the top. **e** Histograms for chromatin density at different time points of the simulation, each corresponding to a column in the zoomed-in graph in panel c. The diamond symbols indicate the maximum of each distribution.

Minor comments:

1. Page 3, line 5: The use of the term 'instead' here is not ideal. Something like 'On the contrary' or 'Conversely' would be more appropriate for the intended message.

Reply: Thank you for your suggestion, we agree and decided to replace 'Instead' with 'Conversely'.

2. In Page 3, line 8, the phrase "Mechanical forces shape chromatin architecture, resulting in histone modifications that influence gene expression and cell fate." Implies a deterministic cause-effect relationship between chromatin architecture changes and histone modifications. Or, a direct and unidirectional path between the two is not supported by evidence. A more appropriate phrase would be: "Mechanical forces alter chromatin architecture, which can enable or modulate histone modifications…".

Reply: Thank you for bringing this to our attention, we completely agree with your comment and we incorporated your statement as suggested.

3. In page 4, at the end of paragraph 2, a reference could be useful in justifying how these specific dimensions reflect physiological constrictions.

Reply: We appreciate your suggestion and we included two references supporting our confinement dimensions. The work by Chen et al. [40] studies endothelial barriers *in vitro* for cancer cell extravasation and describes pore sizes ranging from 1 to 10µm. In addition, Bastianello et al. suggest that pore sizes larger than 3.5µm x 6µm prevent nuclear envelop rupture. Consequently, our 4µm x 6µm constrictions fall perfectly within the described pore sizes in the literature. We included this references in the definition for the geometry of the constrictions:

"The confining regions within the microchannels are defined by semicircular indentations of 8µm in radius, constricting the cross-section up to 4µm at its narrowest point [40]. This pore size is sufficient to cause confinement-induce chromatin changes while preventing nuclear envelope rupture, common in constrictions smaller than 3.5 × 6 μm^2 in cross-section [43]."

[40] Chen, M. B., Whisler, J. A., Jeon, J. S. & Kamm, R. D. Mechanisms of tumor cell extravasation in an *in vitro* microvascular network platform. *Integrative biology: quantitative biosciences from nano to macro* **5**, 1262–1271 (2013).

[43] Bastianello, G. *et al.* Mechanical stress during confined migration causes aberrant mitoses and c-myc amplification. *Proceedings of the National Academy of Sciences of the United States of America* **121**, e2404551121 (2024).

4. Regarding the graphs 2b and 2f: the distribution of pixel intensity in cells during migration is addressed in the paper's text after the measurements regarding the area (figures 2c and 2g). It would thus improve readability if the positions of these were switched in the figure (area plots above the intensity profiles).

Reply: We appreciate your suggestion and understand how the panel positioning might be confusing. Therefore, we modified Figure 2 following your recommendation (see below).

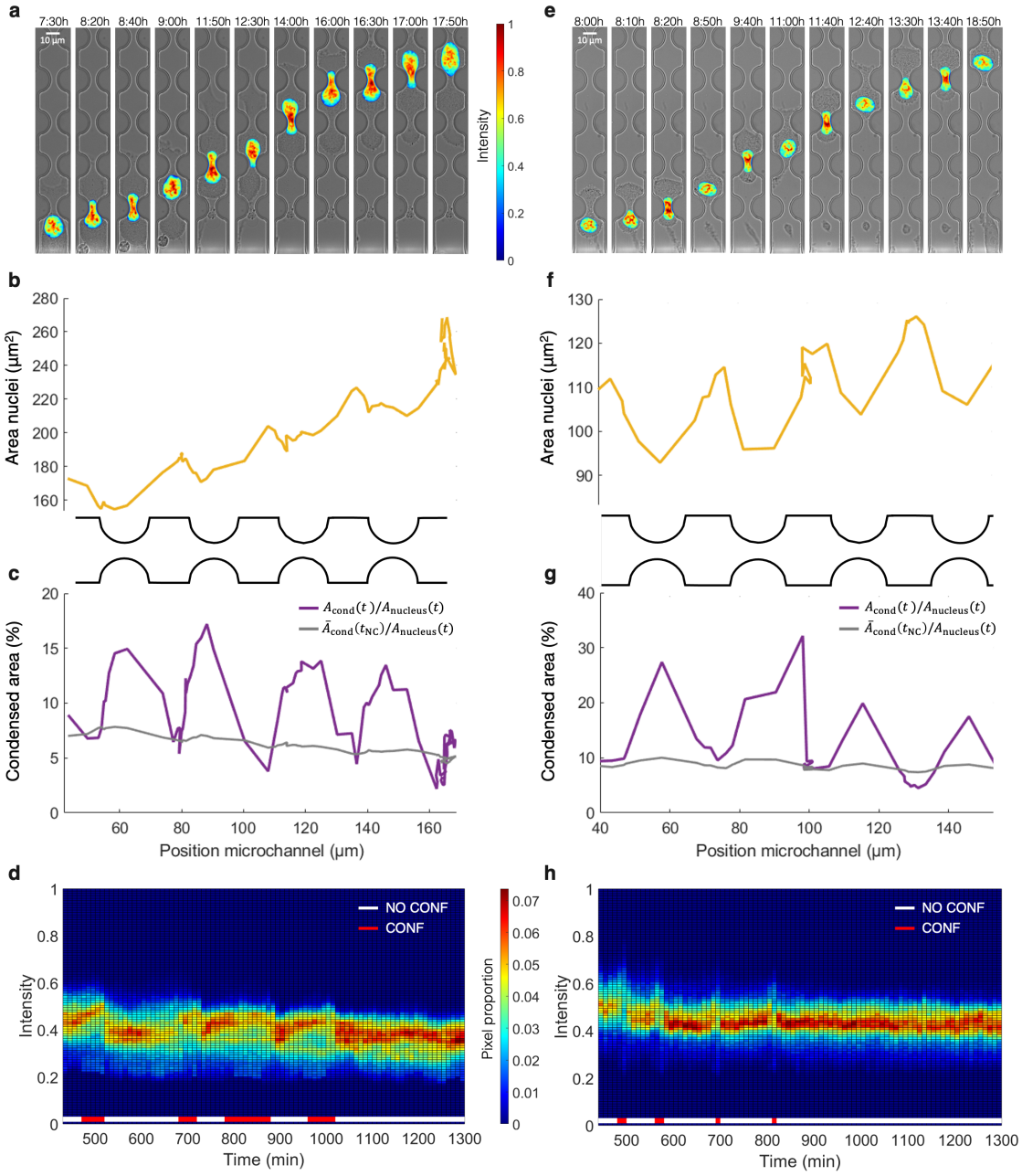

Fig. 2. Single-cell analysis for A549-H2B-GFP cells during migration through periodic confinements in microfluidic devices. a-d Typical results for a representative slow migrating cell. **a** Time-lapse sequence displaying nuclear fluorescence intensity during migration through the microchannel. **b** Evolution of nuclear area plotted against the distance traveled within the channel. **c** Evolution of relative area of the segmented highly-condensed chromatin regions (in purple), i.e. the fraction of the nucleus identified as highly-condensed ($A_{\mathrm{cond}}/A_{\mathrm{nucleus}}$), and basal condensed chromatin content ($\bar{A}_{\mathrm{cond}}(t_{\mathrm{NC}})$) divided by the instantaneous nuclear area ($A_{\mathrm{nucleus}}(t)$) representing the changes in chromatin condensation induced exclusively by changes in nuclear size (in gray). **d** Temporal evolution of the fluorescence intensity profile of the nucleus against time. The line at the bottom of the graph indicates whether the cell lies within a confining region (red) or a non-confining region (white) for the specific frame. **e-h** Similarly, typical results for a representative fast migrating cell. Upon deformation through each of the four confinements, both cells exhibit reversible nuclear shrinking, reversible increase in condensed chromatin area and a distinctive transient dispersion in fluorescence intensity. Note that the minimal increases during confinement in the gray curve for both cells do not explain the peaks in chromatin condensation in purple.

Reply to Reviewer #3

Summary of the work:

In this study, we developed a microfluidic platform composed of alternating confining and non-confining regions, enabling real-time monitoring of chromatin dynamics in individual cells. Our results reveal that nuclear deformation within confined regions leads to a reversible increase in chromatin condensation. Notably, following deformation, condensed chromatin clusters adopt a distinct spatial organization, suggesting incomplete relaxation and thus only partially reversible condensation. Numerical simulations indicate that the interplay between nuclear deformation and attractive interactions among heterochromatin domains may underlie the observed chromatin reorganization. Based on the colledted results, the authors suggest that partially-reversible chromatin condensation acts as an adaptive mechanism in cancer cells to mediate both, gene expression regulation and persistent mechanical memory, which reveals the inherent duality in chromatin dynamics. The study presents compelling results; however, it would benefit from the inclusion of additional, currently missing information and clarification.

Reply: We appreciate the reviewer's constructive feedback and suggestions and have carefully addressed all points raised to improve our manuscript. Below, we provide detailed responses to each specific issue. All changes made to address the comments from Reviewer #3 are highlighted in red in the revised manuscript.

Comments/Questions:

1. Did you notice corrlation between nucleus shape (e.g. circularity, aspect ratio, solidity) and condansation rate after each confinement? It would be worth to include such data.

Reply: We appreciate the reviewer's suggestion. To address this question we analyzed the time-dependent evolution of nuclear morphological features to identify potential trends in our cell population, particularly in nuclear circularity, eccentricity, and solidity. The results are presented in graphs similar to Figure 3, where each data point in a column corresponds to a single cell and represents the average among every frame in which the geometric center of the cell lies within the specified microchannel region, where C1-C5 represent the successive confining regions and N1-N5 represent the non-confining regions following the entry. Note that, contrary to results in Figure 3, data points in these graphs did not need to be normalized with the mean in non-confined regions.

$$\text{Circularity} = \frac{4\pi \times \text{Area}}{\text{Perimeter}^2}$$

Circularity was used to quantify how close nuclear shape is to a perfect circle ($\text{Circularity} = 1$).

$$\text{Eccentricity} = \frac{d}{l}$$

where d is the distance between two foci of the ellipse fitting the nucleus and l is the length of the major axis of the ellipse. Then, 0 corresponds to a perfect circle (both foci coincide at the center) and 1 corresponds to a line segment (extremely elongated ellipse).

$$\text{Solidity} = \frac{\text{Area}}{\text{ConvexArea}}$$

where Area is the number of pixels in the nucleus and ConvexArea is the number of pixels in the convex hull of that region, i.e. the smallest convex shape that can fully enclose the nucleus. Then, $\text{Solidity} = 1$ when the nucleus is perfectly convex and $\text{Solidity} < 1$ if the nucleus is concave or has internal holes, irregular boundaries, or protrusions.

Nuclear circularity and eccentricity point towards smooth rounded nuclei that significantly elongate during confinement. For every constriction, nuclear shape deforms similarly and returns to their original disc-like morphology after confinement. It is noteworthy that solidity in non-confining regions is consistently close to 1, suggesting compact regular nuclei. In confined nuclei solidity decreases, however, the lowest measured values remain considerably higher than those commonly associated with concave, fragmented, or protrusive nuclear morphologies.

To address this comment, Figure R1 has been included in the Supplementary Material with a caption stating briefly the main results. Additionally, this figure has been referenced in Results section 2.1:

"We performed a thorough single-cell analysis to measure quantifiable morphological parameters for each nucleus to characterize its deformation (see Supplementary Figure S3). "

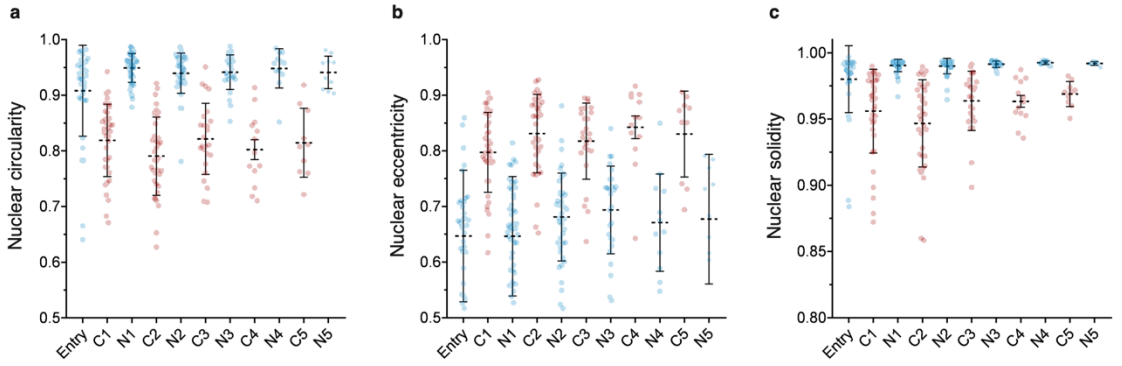

Fig. R1. Cell population analysis for nuclear circularity (**a**), nuclear eccentricity (**b**) and nuclear solidity (**c**) among PACA-H2B-GFP cells migrating through short microchannels. Note that non-confining regions are colored in blue and confinements are in red. These nuclear morphological parameters suggests that nuclei in non-confining regions are characterized by a smooth regular rounded shape. As expected, nuclei elongate during confinement since they exhibit a significantly larger eccentricity. Despite the decrease in solidity for confined nuclei, the minimum value reported is well above those observed in concave, fragmented or protrusive nuclei. These results support that the analysis was conducted on structurally intact and morphologically regular nuclei.

2. "Our analysis revealed that the nucleus area exhibits a sudden drop when entering the confinement for every cell, regardless of their migration speed." Coul you provide a correlation graph and calculation to obsreve the average speed of a cell and normalized nuclei area/condensation area to observe potential differences?

Reply: Thank you for your interesting comment. Following your suggestion, we performed a cell population analysis to generate correlation graphs for migration speed with nuclear area and with highly-condensed chromatin area at the different regions in the microchannel. Each data point in Figure R2 is defined by the mean migration speed and by the mean nuclear area (Figure R2a) or the mean condensed chromatin area (Figure R2b).

Interestingly, migration speed broadens towards higher values during confinement. It is noteworthy that, as expected, the fastest cells are frequently characterized by smaller nuclear areas. Cells larger than 100 μm^2 are restricted to slower migration speeds through the microchannels whereas smaller cells display migration velocities spanning the complete range (see Figure R2a). There is a growing trend in migration speeds within non-confining regions as they are located further downstream, indicating that faster cells migrate deeper into the microchannel channel. Nonetheless, the correlation between migration speed and relative condensed chromatin area does not appear to yield any conclusive pattern.

To include this new analysis in the original manuscript, we added Figure R2 in our Supplementary Material and we modified Results section 2.1 to introduce this correlation:

"Owing to the viscoelastic behavior associated with the cell nucleus in the existing literature [28, 41, 44], we anticipated differences between slow and fast cells. Instead, the evolution of the area of the nucleus depicts a comparable pattern in both groups, characterized by a reversible reduction of the projected nuclear area upon confinement. This suggests that both cell groups migrate at a rate that is much slower than the viscoelastic relaxation time, hence, viscoelastic effects have already relaxed in our quasi-static images of the cell nucleus (10 minutes frame interval). Despite nuclear shrinking being consistent among cells with different migration

speeds, nuclear size did show a correlation with migration velocities (see Supplementary S4). As expected, the fastest cells are frequently characterized by smaller nuclear areas and large cells are restricted to slower migration speeds through the microchannel [43]. Interestingly, migration speed broadens towards higher values during confinement and there is a growing trend in migration velocities within non-confining regions as they are located further downstream, indicating that faster cells migrate deeper into the microchannel. ”

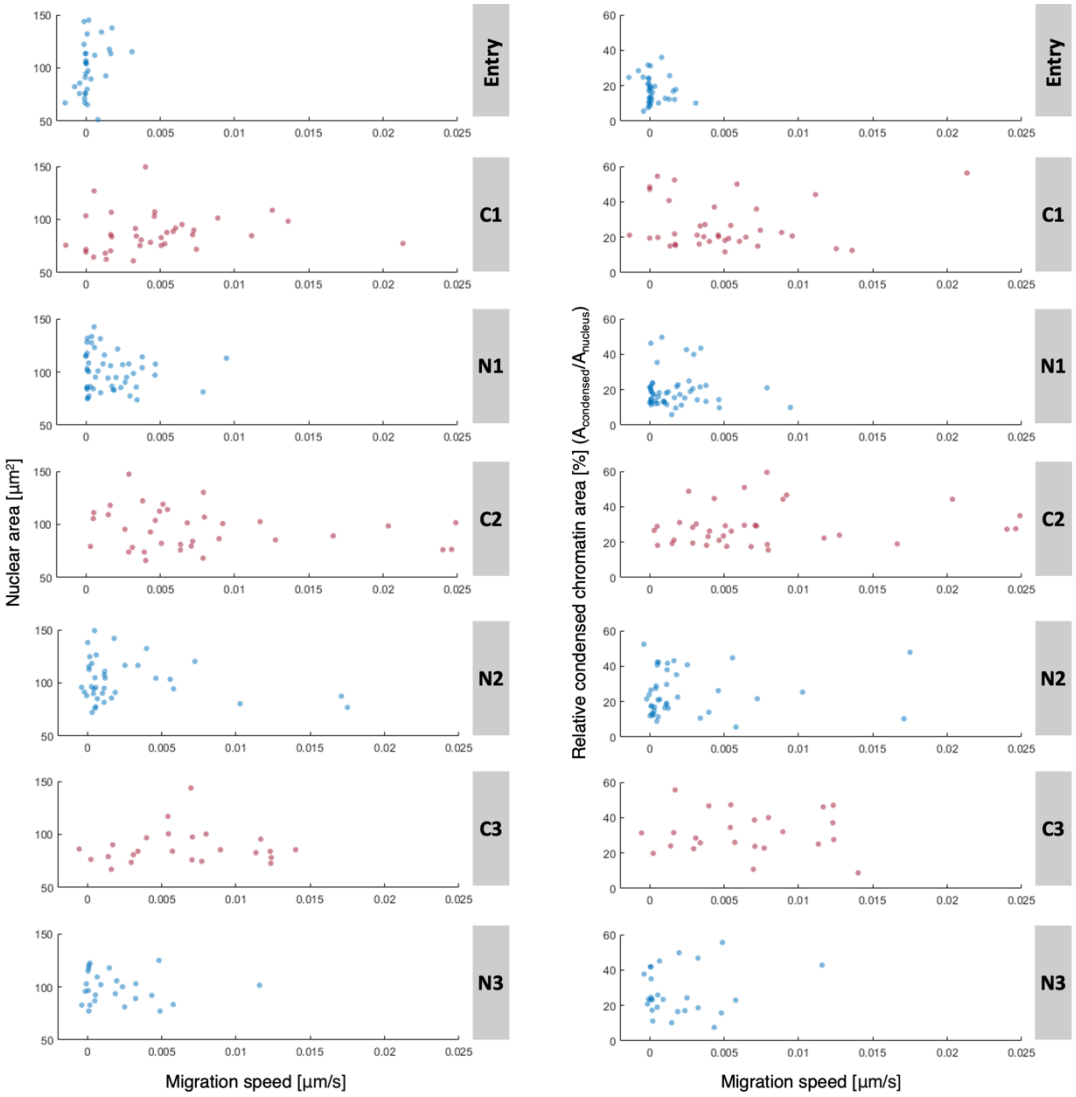

Fig. R2. a Cell population analysis for the correlation of migration speed (x-axis) and nuclear area (y-axis). Each data point is defined by mean speed and mean nuclear area for an individual nucleus within the specific region indicated on the right. Migration during confinement is frequently characterized by a wider distribution towards higher speeds, often corresponding to cells with smaller nuclear areas. **b** Similarly, cell population analysis for the correlation of migration speed (x-axis) and highly-condensed chromatin area over total nuclear area (y-axis). Each data point is defined by mean speed and mean relative condensed chromatin area for an individual nucleus within the specific region indicated on the right. There is not a clear trend for migration speed and chromatin condensation. Note that results for non-confining regions are colored in blue while results for confining regions are colored in red.

3. In the brightfield images of cells migrating through constrictions did you notice that cells migrating facter have a distinc morphological features (e.g. ameboidor elongated cell body)?

Reply: Thank you for your observation. We did not notice relevant morphological features for fast cell migration in the brightfield images. The great majority of cells exhibited a similar morphological deformation of the nucleus during migration. An example for the circularity and the eccentricity of a representative fast cell can be found in Figure R3. Note that this cell corresponds to cell in Figure 2e-h in the manuscript. The pattern and the range for these parameters is consistent with the results for the cell population (Figure R1).

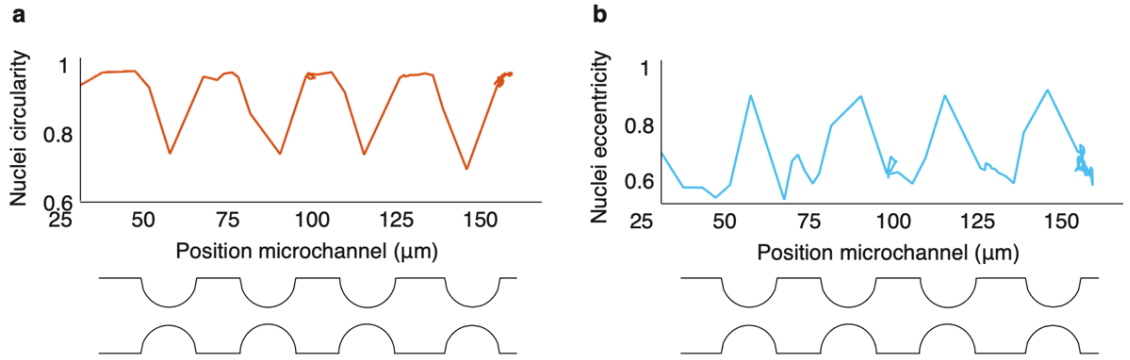

Fig. R3. Single-cell analysis for nuclear circularity (**a**) and for nuclear eccentricity (**b**) in a representative fast PACA-H2B-GFP cell migrating through short channels. Note that the pattern and the range for these parameters is consistent with the results for the cell population.

4. Cells traveled longer distances trought short channels than in long channels as depicted in the Figure 3 and Supplementary Material Sec. S3. Could you speculate why was it happening, was it associated with e.g. higher nuclear envelope rupture or DNA damage?

Reply: Thank you for your comment, we appreciate the opportunity to elaborate further on this point. Nuclear envelope rupture throughout every experiment was scarce, instead we believe that the differences in migration lengths are mainly due to the distances between successive confinements. In short channels, non-confining intervals are smaller leading to a reduced spacing between adjacent confinements. In these channels the cytoplasm of the cell during migration is able to reach further into the following confinement, which seems to promote faster translocation of the nucleus through successive constrictions. Additionally, reduced non-confining segment lengths results in prolonged confinement of the cytoplasm, which could potentially act as a mechanical signal to accelerate cell migration.

We decided to include a statement in Results section 2.1 acknowledging these confining features in short channels:

“The results for both long and short microchannels, in terms of the analyzed nuclear features, were strikingly similar; indeed, the only observable difference was that more cells migrated through short channels and traveled longer distances than in long channels. Greater migration lengths in short channels could potentially be favored due to the proximity between adjacent constrictions and the prolonged confinement of the cytoplasm, which remains constricted even in non-confining regions.”

5. In Bastianello et al., 2024 (PMID: 38990945), in both utilized cell lines U2OS and HeLa, the speed of migration across constrictions increased linearly with the nuclear size, suggesting a direct relationship between cell cycle, size, and speed. Did authors observe such correlation? Furthemore, in Bastianello et al., 2024 (PMID: 38990945) the authors observed that migration across constrictions can significantly delay cell cycle progression, was it also seen in this manuscript, what was division rate in the cell lines that you analyzed? Were there any differences between short and long channels?

Reply: Thank you for your careful consideration of this matter. We did not directly quantify the relationship between cell cycle, nuclear size and migration speed since we mainly focused on measuring chromatin condensation dynamics. On the statement from Bastianello et al. there appears to be an erratum, the speed across constrictions 'decreases' with nuclear size as shown in their Figure 1(A) where larger time periods are required for cells in the G2 phase to traverse the confinement.

Nevertheless, we did observe nuclear shrinking during confinement which appears to trigger cell cycle arrest. More specifically, cells undergoing rapid, repetitive confinement did not show an increase in nuclear size, contrarily, nuclear enlargement was only observed in cells that spent sufficient time in non-confined conditions. Therefore, nuclear growth associated with cell cycle progression was restricted exclusively to those cells that remained unconfined long enough. This cell cycle arrest aligns with the results of Bastianello et al. in delayed cell cycle.

We agree with the reviewer that measuring cell division rate could yield an interesting analysis. Unfortunately, the complex cell tracking algorithm required to analyze cell migration in our high-throughput experimental configuration limits our availability to quantify cell division. In our experiments, mitotic cells were not considered by excluding from the analysis 20 frames (200 minutes) before and after cell division. Consequently, measuring differences in cell division rate between short and long channel is not within the scope of our project. Nonetheless, future work will include post-mitotic cell tracking, which could provide additional insights into persistent chromatin changes maintained after cell division.

Accordingly, we have referenced Bastianello et al. to support our observation of cell cycle arrest and we have included measuring cell division rate as future work in the Discussion section:

"Additionally, we noted that the nucleus area often exhibits not only a recovery of its original area but also a growing tendency after crossing a confinement. In fact, this event was observed in most cells except for a few cases displaying rapid migration. These particular cells migrated fast through both the constrictions and the non-confining segments of the channel. Therefore, cells that spend sufficient time in the non-confining regions, regardless of their speed to traverse the constrictions, show a noticeable increase in the nucleus area with time. Nuclear growth is probably related to the progression of the cell cycle. The volume of the cell nucleus increases as the cell approaches mitosis and slower cells had more time to progress through their cell cycle as they traversed the channels, hence, they frequently exhibit greater total nucleus growth than fast cells [20, 42]. Consequently, fast cells lacking nuclear growth suggest that prolonged confinement leads to cell cycle arrest or delayed cell cycle progression as described by Bastianello et al. [43]"

"Future studies should aim at single-cell sequencing to unravel how the deformation triggers specific chromatin states and epigenetic marks and should employ higher-resolution or real-time imaging techniques to capture finer-scale chromatin dynamics. Additionally, tracking daughter cells after mitosis could reveal interesting confinement-induced chromatin changes stably maintained beyond cell division, which may be related to potential metastatic regulators."

6. As it was published that confined migration increases H3K9me3 and H3K27me3 heterochromatin marks that could persist for long time (Chieh et al., 2022, PMID: 36117991), the authors observed correlation between facultative heterochromatin loci (H3K27me 3 marker), which have been shown to increase more than constitutive heterochromatin (H3K9me 3 marker) upon confined migration. Was the total area of both markers H3K9me3 and H3K27me3 (both separate and merged) increased during passage through the constriction and after? Please perform such analysis.

Reply: We thank the reviewer for this interesting suggestion. We agree that performing a quantitative, time-dependent analysis of heterochromatin evolution would add significant value to our study. Nevertheless, our current experimental setup imposes practical constraints.

To identify heterochromatin loci within cell nuclei, we fixed the cells after 24 hours of migration and performed immunostaining using two well-characterized heterochromatin markers, H3K9me3 and H3K27me3. The confining microchannels, however, generate a complex diffusion gradient of the staining reagents, which results in nonuniform marker distribution when multiple cells occupy a single channel. As a result, suggesting a time-dependent evolution of chromatin requires accounting for diffusion-related variability and comparing cells located at different positions along the microchannel. To mitigate these diffusion effects, introducing a complementary euchromatin marker such as H3K9ac could be done to compute a heterochromatin-to-euchromatin ratio which is then normalized among cells. Nonetheless, our cell line expresses intrinsic nuclear GFP, which limits the availability of laser lines for additional fluorophores and prevents simultaneous imaging of H3K9me3, H3K27me3, and H3K9ac in a single sample.

To acknowledge this limitation and highlight their relevance in future analysis, we referenced Hsia et al. (PMID: 36117991) and included the following statement in the Discussion of the manuscript:

"Despite this improved time-lapse interval (one frame every 10 minutes), our temporal resolution is not sufficient to capture rapid enzyme-mediated heterochromatin dynamics. Another limitation of our study arises from intercellular variability during the heterochromatin loci analysis. To identify heterochromatin domains within cell nuclei, cells were stained for two well-established heterochromatin markers, H3K9me3 and H3K27me3. However, the confining microchannels used in our experiments generate complex diffusion gradients of the staining reagents, leading to nonuniform marker distribution when multiple cells occupy the same channel. This effect introduces additional variability that constraints the precision of quantitative comparisons across nuclei. To compensate for diffusion-related variability, future analyses could include a complementary euchromatin marker (e.g., H3K9ac) to normalize staining by computing the heterochromatin-to-euchromatin ratio in each cell. Addressing this limitation in the future could be interesting to study the evolution of persistent heterochromatin marks as the cells migrate further in the microchannel [30]. Future studies should aim at single-cell sequencing to unravel how the deformation triggers specific chromatin states and epigenetic marks and should employ higher-resolution or real-time imaging techniques to capture finer-scale chromatin dynamics."

7. In Figure 5b authors present a bar chart representing the spatial correlation coeffcient for chromatin distribution (green) against each heterochromatin marker (magenta and cyan), classified according to the confined state of the cell: confined or non-confined. It is not clear for me how the bar chart was genererated. Was it based on the images from Fig. 5a or a population of cells (which would be preferential). Which correlation coefficient was used (e.g. Pearson's)? Please provide also a scatter plots to visualize the correlation.

Reply: We thank the reviewer for bringing this point to our attention, which prompted us to elaborate further. The bar chart is generated based on the data from 18 confined PACA-H2B-GFP cells and 123 non-confined PACA-H2B-GFP cells. For spatial correlation, we computed the 2D correlation coefficient by implementing the MATLAB function *corr2*, which is based in Pearson's correlation coefficient:

$$r = \frac{\sum_i \sum_j (A_{ij} - \bar{A})(B_{ij} - \bar{B})}{\sqrt{[(\sum_i \sum_j (A_{ij} - \bar{A})^2)(\sum_i \sum_j (B_{ij} - \bar{B})^2)]}}$$

where $\bar{A}$ is the mean among all values in image array A and $\bar{B}$ is the mean among all values in image array B.

Following the reviewer's recommendation, we have modified Figure 5 to include the scatter plot (Figure R4a) and the sample size in the caption. Additionally, we have introduced the following statement in Methods section 4.7:

"Heterochromatin content and distribution were analyzed using ImageJ to segment individual nuclei and, then, MATLAB to quantify fluorescence intensity among other parameters of interest. To measure the spatial correlation of heterochromatin markers and GFP signal, MATLAB function *corr2* was implemented. This function is based on Pearson's correlation coefficient applied to all the elements in the array defining the nucleus fluorescence image."

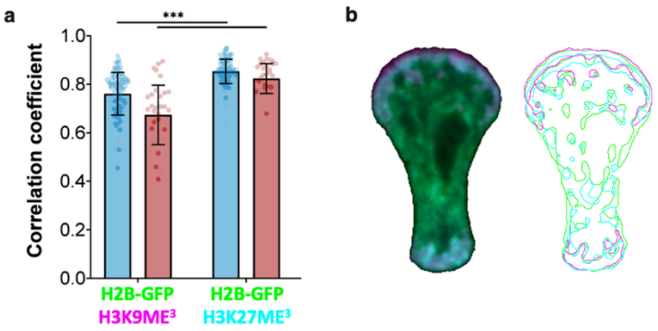

Fig. R4. a Spatial correlation for chromatin distribution (green) against each heterochromatin marker (magenta and cyan), classified according to the confined state of the cell: confined (n=18) or non-confined (n=123). **b** Merge of the fluorescent channels for a representative confined cell (left) and overlap of the segmentation outcome for the three fluorescent channels (right). The correlation coefficients for this cell between H2B-GFP signal and the heterochromatin markers are 0.79 for H3K9me^3 and 0.90 for H3K27me^3.

8. It is known that some proteins can accumulate in the front of cell's nucleus during confined migration, e.g. Nesprin-2 (PMID: 32419336, PMID: 40340251), potentially thethering heterochromating towards them. Did you observe increased heterochromatin markers towards the front of the nucleus when compared to the rear?

Reply: We thank the reviewer for this insightful comment. Together with the limitations of the immunofluorescence assay described in question 6, the use of fixed cells prevents reliable quantification of heterochromatin domain localization at different time points during confined migration. Nevertheless, the notably high correlation coefficient between heterochromatin markers and condensed chromatin cluster segmentation prompt us to measure cluster distribution along the direction of the microchannel, aiming to detect a preferential accumulation of chromatin clusters at the front or the rear of the nucleus. We performed a population analysis of the distance between the center of mass of the nucleus and its geometric center (centroid).

The center of mass corresponds to the intensity-weighted centroid of the nucleus, i.e. the point representing the average position of fluorescence signal across all pixels. It represents the coordinates where the intensity would "concentrate" if the signal were treated like physical mass. Formally, for an image where each pixel (x, y) has an intensity value $I(x, y)$:

$$x_{CM} = \frac{\sum(x \cdot I(x,y))}{\sum I(x,y)}, \quad y_{CM} = \frac{\sum(y \cdot I(x,y))}{\sum I(x,y)}$$

The geometric center is calculated as the arithmetic mean position of all the pixels in the nucleus. It consists of adding the pixels x-coordinates and dividing by the number of pixels to get the centroid x-coordinate and accordingly for the centroid y-coordinate:

$$x_{\text{centroid}} = \frac{1}{n}\sum_{i=1}^{n} x_i\,, \quad y_{\text{centroid}} = \frac{1}{n}\sum_{i=1}^{n} y_i$$

Then, we subtracted the centroid from the center of mass along the y-coordinate, which aligns with the direction of the microchannels. Therefore, a positive value implies chromatin accumulation at the front of the cell while a negative value indicates chromatin accumulation at the rear of the cell. Nevertheless, the results were not consistent with a preferential accumulation of chromatin clusters on one side of the cell. The distance from the centroid to the center of mass along the y-axis is minimal and a distinctive trend with successive confinements towards positive or negative values was not detected (see Figure R5).

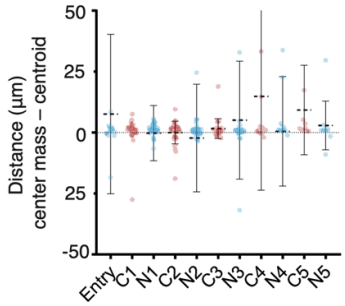

Fig. R5. Cell population analysis for the vertical distance between the intensity center of mass and the geometric center of the nucleus. The center of mass represents the average position of fluorescence signal across all pixels. Positive distance values indicate that the intensity center of mass lies at the front of the cell (before the geometric center) while negative values indicate that it lies at the rear of the cell (after the geometric center).

To include briefly the results of this analysis, we added the following statement at the end of Results section 2.5, where we explore chromatin cluster distribution in the nucleus:

"Some proteins, such as Nesprin-2 [49, 50], have been shown to accumulate at the front of the cell during confined migration. To explore whether chromatin clusters accumulate preferentially at the front or the rear of the nucleus during successive confinements, we performed a cell population analysis considering the spatial distribution of these clusters. The distance between the center of mass, i.e. intensity-weighted centroid of the nucleus, and the geometric center of the nucleus along the direction of the microchannel was used to estimate if the location where fluorescence intensity concentrates lies at the front or the rear of the nucleus. Nevertheless, the results were not consistent with a preferential accumulation of chromatin clusters on one side of the nucleus (see Supplementary Figure S8). The distance from the center of mass to the geometric center along the microchannel direction is minimal and it does not exhibit a distinctive trend towards positive (accumulation at front) or negative (accumulation at rear) values."

Accordingly, we included the methodology at the end of Methods section 4.6:

"In addition, a population analysis of the distance between the center of mass of the nucleus and its geometric center (centroid) was performed to estimate the location where chromatin clusters preferentially accumulate.

The center of mass corresponds to the intensity-weighted centroid of the nucleus, i.e. the point representing the average position of fluorescence signal across all pixels. It represents the coordinates where the intensity would "concentrate" if the signal were treated like physical mass. Formally, for an image where each pixel (x, y) has an intensity value $I(x, y)$:

$$x_{CM} = \frac{\sum(x \cdot I(x,y))}{\sum I(x,y)}, \quad y_{CM} = \frac{\sum(y \cdot I(x,y))}{\sum I(x,y)}$$

The geometric center is calculated as the arithmetic mean position of all the pixels in the nucleus. It consists of adding the pixels x-coordinates and dividing by the number of pixels to get the centroid x-coordinate and accordingly for the centroid y-coordinate:

$$x_{centroid} = \frac{1}{n}\sum_{i=1}^{n} x_i\,, \quad y_{centroid} = \frac{1}{n}\sum_{i=1}^{n} y_i$$

Then, we subtracted the centroid from the center of mass along the y-coordinate, which aligns with the direction of the microchannels. Therefore, a positive value implies chromatin accumulation at the front of the cell while a negative value indicates chromatin accumulation at the rear of the cell."

9. Confined migration can lead to increase nuclear envelope rupture events (PMID: 27013428). What was the nuclear envelope rupture rate in the conditions? Did you see any correlations between the chromatin condensation and NE rupture rate? How about the NE rupture rate after multiple passages?

Reply: We appreciate this careful observation. NE rupture throughout our experiments was scarce, thus, the sample size would be insufficient to yield reliable results. We engineered our confining microchannels to subject the cells to sufficient deformation to observe confinement-induced chromatin changes (Hsia et al. 2022) while preserving nuclear integrity with constrictions larger than 3.5 × 6 μm^2 in cross-section (as suggested by Bastianello et al. 2024).

To clarify in the manuscript that NE was scarce we added the following statement when describing the design of the microchannels in Methods 4.1 and the analysis in Methods 4.5:

"The confining regions within the microchannels are defined by semicircular indentations of 8μm in radius, constricting the cross-section up to 4μm at its narrowest point. This pore size is sufficient to cause confinement-induce chromatin changes while preventing nuclear envelope rupture, common in constrictions smaller than 3.5 × 6 μm^2 in cross-section [43]."

"Following successful alignment, a cell tracking code was developed to identify the nuclei path across the imaging sequence and to determine the state of the cell nuclei, confined or non-confined. For the analysis three different zones were distinguished in the microchannels (see Figure 3a), the non-confining regions, the confining regions and a transition zone in between the former two in which the results are not considered for the cell population analysis. Although nuclear envelope rupture plays a significant role during confined migration [58], the constriction sizes in our experiments maintained nuclear integrity [43], resulting in rare rupture events. Cells with compromised nuclear envelopes, identified by cytoplasmic GFP and nuclear blebs, were excluded from analysis."

Reply to Reviewer #4

Summary of the work:

This well-written manuscript uses H2B-GFP–expressing cells and a microfluidic device to investigate chromatin dynamics during and after confined migration. The authors show that chromatin compacts as the nucleus transits through confinement and partially recovers after exit, but does not fully return to the pre-migration state. Notably, the distribution of condensed chromatin region sizes broadens following confinement, suggesting lasting changes in chromatin organization. Coarse-grained polymer simulations, excluding biochemical factors, further demonstrate that the observed behavior can be explained by purely physical chromatin reorganization. This work is timely, given the increasing interest in how confinement affects nuclear structure and function.

However, several major concerns need to be addressed before considering this manuscript for publication.

Reply: We would like to thank the reviewer for their time and insightful comments, which have helped to improve the quality of our manuscript. Below, we provide detailed responses to each specific issue raised by the referee. All changes made to address the comments are highlighted in red in the revised manuscript.

Major Points

1. Sample size in Figure 2: Results are currently based on two cells (one slow and one fast migrating). Data from additional cells are necessary to establish reproducibility, particularly since this figure underpins the claim that confinement increases chromatin condensation range ("dispersion in pixel proportion towards opposing ends").

Reply: Thank you for raising this concern, this point was not clear in the previous version of the paper. Our single-cell analysis involved more than 100 cells, each examined individually to study the evolution of multiple variables of interest, particularly, the nucleus fluorescence intensity profile, the nucleus area and the highly-condensed chromatin content. The resulting graphs are straightforward to interpret and enable assessment of both temporal and spatial changes in these variables. From the outset of the single-cell analysis, we detected significant confinement-related changes in these variables, with a consistent pattern observable in every cell. Consequently, we performed a population level analysis where we validated these evolutionary trends across the cell population by normalizing variables for each cell to track their progression along the microchannel (Figure 3).

The two cells displayed in Figure 2 are just some representative examples of the A549-H2B-GFP cells analyzed. Similarly, we included in our supplementary files another two representative examples of the single cell analysis for PACA-H2B-GFP cells (Fig. S2).

We hope that this explanation clarified your comment, and we included the following statement in section 2.1 of the manuscript:

"We performed a thorough single-cell analysis, involving more than 100 migrating cells, to measure quantifiable morphological parameters for each nucleus to characterize its deformation (see Supplementary Figure S3). The evolution of the parameters of interest was studied as a function of the position of the geometric center of the nucleus within the microchannel. The results for two representative cells are displayed in Figure 2."

2. Nuclear size correlation: In Figure 2, migration speed appears correlated with nuclear size. This relationship should be discussed, and subsequent analyses (Figure 3-5) should stratify cells by migration speed and nuclear size. Analysis of condensed area vs. nuclear area dynamics during confinement would be especially informative.

Reply: We appreciate your observation, and we agree that migration speed and nuclear size are correlated, however, we excluded their relationship from the scope of our analysis. Instead, we did study how migration speed influences chromatin condensation and found that the pattern in chromatin condensation was consistent between fast and slow cell populations. We decided against stratifying the data based on migration speed or nuclear size because our objective was to capture global population trends after analyzing each cell individually. Nevertheless, we did consider nuclear size during our population level analysis, each data point is normalized with the average area of the nucleus during non-confined migration.

We agree that analyzing condensed chromatin area vs. nuclear area dynamics could be informative. Therefore, we decided to modify Figure 2d,h to include a plot for basal condensed chromatin as a function of nuclear area for each frame:

$$y(t) = \frac{\bar{A}_{\text{condensed}}(t_{NC})}{A_{\text{nucleus}}(t)}$$

where $\bar{A}_{\text{condensed}}$ is the average highly-Condensed Chromatin area among the frames in which the cell is unconfined (t_{NC}), i.e. during all non-confining regions Entry, N1, N2…, and $A_{\text{nucleus}}(t)$ is the nuclear area in frame t.

Then, $y(t)$ represents the changes in condensed chromatin area attributed exclusively to fluctuations in nuclear size (see the gray curve in Figure R1b). This plot also allows us to demonstrate that nuclear shrinking is not sufficient to explain our peaks in chromatin condensation upon confinement (purple curve in Figure R1b).

Accordingly, we modified the figures and we added the following statement in the original manuscript in Results Section 2.2:

"After deformation, the nucleus recovers its basal chromatin condensation state which generally lies around 5 to 10% of the total nucleus area. Note that the twofold to threefold increase in highly-condensed chromatin area cannot be explained by the decrease in nuclear area upon confinement. To represent the contribution of nuclear shrinking in the quantification of chromatin condensation, the gray line in Figure 2c,g displays basal condensed chromatin content divided by the instantaneous area of the nucleus. Basal condensed chromatin represents the mean highly-condensed chromatin area of the nucleus averaged over all non-confining regions (Entry, N1, N2…). Then, its evolution along the microchannel (gray curve) illustrates the changes in chromatin condensation induced by changes in nuclear area only. The notably limited growths during confinement do not to explain the peaks in the segmentation of condensed chromatin area (in purple in Figure 2c,g)."

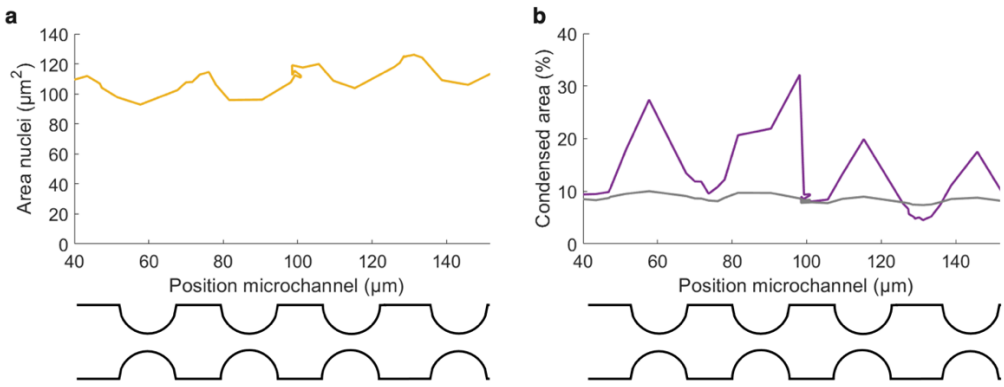

Fig. R1. a Evolution of the nucleus area for a representative A549-H2B-GFP cell migrating through short confining microchannels. **b** Evolution of the relative highly-condensed chromatin area representing the percentage of the nucleus segmented as condensed chromatin (purple) and the evolution of basal condensed chromatin content in non-confined regions as a function of nuclear area for each frame (gray).

3. Cell cycle state: Chromatin compaction and nuclear size are cell-cycle dependent. The authors should consider DNA replication block (e.g., thymidine treatment) to control for this.

Reply: Thank you for your careful consideration of this matter. We agree that chromatin compaction and nuclear size are cell-cycle dependent and relevant for the analysis. However, we decided not to use cell-cycle control treatments because our goal was to observe the native cellular response to confinement without external interference. Intervening in cell cycle progression could obscure important biological insights. For example, we observed cell cycle arrest during confinement: cells undergoing rapid, repetitive confinement did not show an increase in nuclear size, contrarily, nuclear enlargement was only observed in cells that spent sufficient time in non-confined conditions.

To minimize confounding our results with chromatin condensation effects attributed to mitosis, we excluded from the analysis 20 frames (200 minutes) before and after cell division. Furthermore, to evaluate chromatin changes independently of the cell cycle, we normalized our variables by nuclear area, particularly when measuring highly-condensed chromatin areas, thereby accounting for nuclear size variations and ensuring accurate assessment.

To provide clarity on this issue, the following statement was included in Methods Section 4.5:

"Following successful alignment, a cell tracking code was developed to identify the nuclei path across the imaging sequence and to determine the state of the cell nuclei, confined or non-confined. For the analysis three different zones were distinguished in the microchannels (see Figure 3a), the non-confining regions, the confining regions and a transition zone in between the former two in which the results are not considered for the cell population analysis. Although nuclear envelope rupture plays a significant role during confined migration [58], the constriction sizes in our experiments maintained nuclear integrity [43], resulting in rare rupture events. Cells with compromised nuclear envelopes, identified by cytoplasmic GFP and nuclear blebs, were excluded from analysis. It is also noteworthy that to prevent considering chromatin condensation effects attributed to mitosis while avoiding the use cell-cycle control treatments that might interfere with native chromatin dynamics, we excluded from the analysis 20 frames (200 minutes) before and after cell division.".

4. Clarification of "dispersion in pixel proportion": More explanation is needed. The intensity range seems stable, while the peak broadens, implying that the pixel intensity gets distributed within a constant range. Is this interpretation correct? The current description seems to imply that the intensity range (intensity min/max) increase with confinement.

Reply: Thank you for bringing this to our attention. We agree that further clarification is necessary and apologize for any previous unclear explanation. We have revised the text accordingly to improve clarity and accuracy in section 2.3:

"Fluorescence intensity histograms over time often display large fluctuations in the pixel values during non-confining regions, which adds noise to the analysis (Figure 2d,h). We observed that alterations in the fluorescence intensity profile upon the nucleus deforming through a confinement are highly heterogeneous among different cells. Yet, the fluorescent histograms depict a distinctive distribution in pixel proportion towards opposing ends of the intensity range whenever the cell traversed a confinement. Note that the intensity range is fairly constant during the analysis but, interestingly, the number of pixels with the highest and the lowest intensity levels increased simultaneously upon deformation (Figure 2d,h)."

5. Image analysis transparency: The methods mention MATLAB processing, but the actual code and detailed description of the algorithm (e.g., which adaptive filter was used) should be included. This would enhance reproducibility and serve as a resource for the community.

Reply: We appreciate your suggestion and we agree that the MATLAB processing code should be more thoroughly explained. To address this comment, we modified the Methods section 4.6:

"Finally, a custom MATLAB script implementing an adaptive image filter was used to compute the binary mask that identifies highly-condensed chromatin regions. This algorithm excludes pixels with intensities lower than 0.6 (normalized intensity) and it relies on the MATLAB function *adaptthresh* to select specific thresholds for the segmentation according to local mean intensity in neighboring

pixels. Similar segmentation algorithms using this MATLAB function have already been described in the literature [59-61].”

Please note that the segmentation algorithm was already included in the data availability statement as a resource for the community (https://github.com/yablazro/Segmentation-chromatin-clusters). The code is accordingly commented to guide the user through the imaging post-processing options.

6. “Spatial distribution” terminology: Section 2.5 and other areas use this phrase, but quantification appears limited to size distribution. Size distribution does not reflect spatial distribution; please clarify.

Reply: We appreciate your observation. Even though our computational simulation shows spatial reorganization of chromatin clusters which fuse during confinement (see Supplementary Video S2), we did not prove this rearrangement experimentally. Consequently, we agree that using the term “spatial distribution” is misleading in this context. The manuscript has been modified to replace “spatial distribution” with “size distribution” accordingly.

7. Sample size reporting: Numbers of analyzed nuclei are missing for Figures 4B–C and 5B. Please include sample sizes, define error bars (SD vs. SEM), and provide correlation coefficients for Figures 5E and 5H (as a representative value against the bar plot in 5B).

Reply: Thank you for pointing this out. Figure 4b includes 65 cells and Figure 4c includes 42 cells, these are the same cells that were concerned in the population level analysis (Figure 3). For Figure 5b, 18 confined cells and 123 non-confined cells were analyzed, and the error bars represent the standard deviation. Additionally, we agree that including the correlation coefficients for Figure 5e,h could be helpful when interpreting the results. Correlation coefficients for Figure 5e are 0.79 for H3K9me^3 marker and 0.90 for the H3K27me^3 marker. Correlation coefficients for Figure 5h are 0.64 for H3K9me^3 marker and 0.85 for the H3K27me^3 marker. The captions for both figures have been modified to address these issues in the original manuscript.

8. Cluster number dynamics: The manuscript states that confinement brings heterochromatin regions closer, leading to persistent interactions. If true, the number of condensed regions should decrease during migration. Please quantify cluster number dynamics, which would also support the discussion statement that “small clusters disappear to form larger clusters.”

Reply: We sincerely appreciate this insightful comment. Following your suggestion, we conducted a complementary analysis that strengthens the results in our manuscript. To quantify the number of chromatin clusters in every cell throughout all frames we generated individual histograms for each microchannel region, similar to those in Figure 4. Each histogram represents the normalized count (bin count over the total number of counts) for the number of chromatin clusters inside a nucleus within successive regions in the microchannel, non-confining regions in blue and confining in red.

These distributions indicate that, prior to migration through confinement, most cells predominantly display 5–10 chromatin clusters (see Figure R2). Upon entering confinement, cells tend to exhibit fewer clusters, aligning with our results for larger cluster sizes due to chromatin compaction during deformation. After exiting confinement, the distribution broadens again toward higher cluster numbers. However, as cells experience repetitive confinement cycles, lower cluster counts (typically

1–5 per cell) become progressively favored. According to the possible compaction mechanisms suggested for confined migration in our original manuscript:

“Other protein condensates have been seen to fuse during confined cell migration [13, 18], hence, we wondered whether dense chromatin clusters (1) aggregate into larger domains via coalescence, (2) expand as individual units, or (3) form new clusters of highly-condensed chromatin.”

these findings are consistent with chromatin cluster aggregation. Chromatin clusters tend to merge and grow in size during confinement. After deformation, some regions separate into individual clusters and revert to their initial state, whereas others remain fused, leading to an overall shift toward fewer but larger clusters.

Consequently, we have modified Figure 4 in the manuscript to include the distributions of chromatin cluster number (Figure 4c) for PACA-H2B-GFP cells together with the distribution of chromatin cluster size, already in Figure 4b. The caption for Figure 4 has also been revised and the following statement was added in Results section 2.5:

“To study the evolution of condensed chromatin clusters upon the nucleus deformation through the confinement, we analyzed the distribution of the areas for individual condensed chromatin clusters and of the total cluster number per nucleus.

…

Therefore, each column in the histogram represent the normalized number of clusters of a relative area that appear among all nuclei and all time steps in the experiments for a specific region. Note that the histograms are normalized with the total number of counts, therefore, the vertical axis represents the probability for the cluster sizes in the horizontal axis. Similar distribution plots were calculated for the number of condensed chromatin clusters in every nucleus throughout the migration experiment. These charts allowed us to capture population-level trends rather than focusing solely on single-cell differences.

…

Studying the distribution of cluster number allowed us to deepen further on the condensation mechanism for chromatin domains. Prior to migration through confinement, most cells predominantly display 5–10 chromatin clusters (see Figure 4c). Upon entering confinement, cells tend to exhibit fewer clusters and, after exiting the constriction, the distribution broadens again toward higher cluster numbers. Nevertheless, as cells experience repetitive confinement cycles, lower cluster counts (typically 1–5 per cell) become progressively favored. This distribution pattern is consistent with chromatin cluster aggregation upon confined migration. During deformation, chromatin clusters come into proximity and tend to merge. They grow in size and, after confinement, some regions separate into individual clusters and revert to their initial state, whereas others remain fused, leading to an overall shift toward fewer but larger clusters. This explanation accounts for the simultaneous increase in cluster size and reduction in cluster number.”

Note that the corresponding analysis for A549-H2B-GFP cells has now been incorporated in the Supplementary Material.

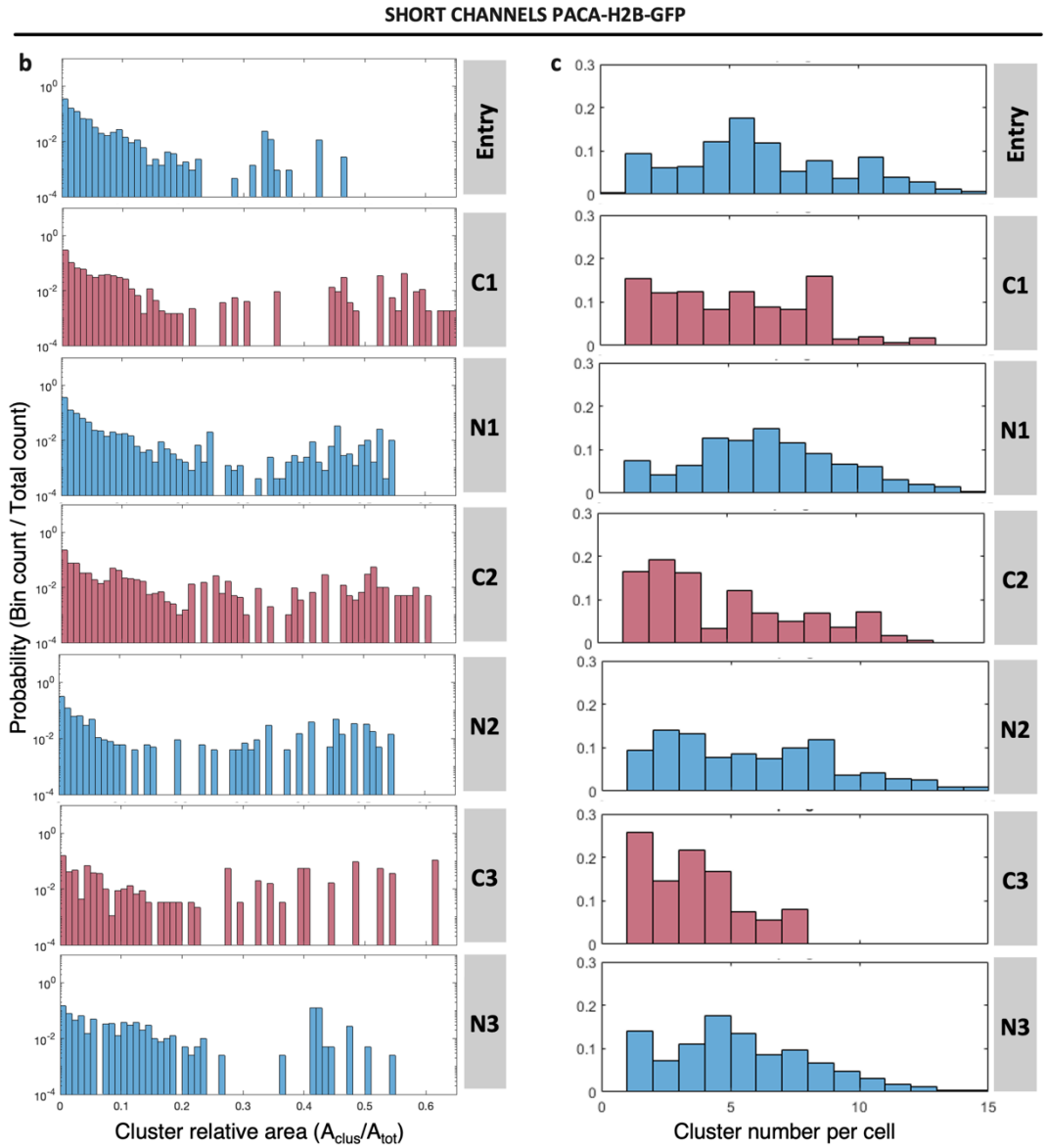

Fig. R2. a Schematic on how to quantify areas for condensed chromatin clusters. **b** Histograms to study the distribution of the area for individual highly-condensed chromatin clusters, which were segmented according to nucleus fluorescence for PACA-H2B-GFP cells in short channels. From top to bottom, each graph corresponds to a different microchannel region, either non-confining (in blue) or confining (in red), and contains the relative area for every chromatin cluster in each cell during all frames in which the cell lies within the corresponding region. The counts for the condensed chromatin clusters in each cell are normalized to 100 data points to avoid misrepresenting cells that migrate faster through the microchannels. **c** Similarly, histograms to study the distribution of the number of individual chromatin clusters for PACA-H2B-GFP cells in short channels. **d** Complementary illustration of the nucleus of a cell migrating through a microchannel with the segmentation of condensed chromatin clusters as an example to represent condensed chromatin cluster dynamics.

Minor Points

9. "We identified two distinct behavioral patterns, one associated with slow cells and the other with fast cells. The former comprises cells that traverse the confinement in less than 40 minutes, whereas the latter includes cells requiring a longer time to complete the traversal." – The sentence describing migration speed patterns is flipped—fast vs. slow cells are mislabeled.

Reply: Thank you for pointing this out. We corrected the labeling in the original manuscript.

10. All microscopy images should include scale bars.

Reply: Thank you for bringing this to our attention. Figures 2a,e and Figure 5a now include their corresponding scale bars.

11. In Figure 2, panels B and F are referenced later in the text; consider repositioning them. Their legend should also explain the red bar (presumably confinement). Panel H is missing its label.

Reply: We are grateful for your feedback. We agree that repositioning panels b and f in Figure 2 improved the clarity of the figure, and we also included the missing label and the legend you suggested.

12. Fig. 3B and C, what are the data normalized to? Why the data is not 1 at entry? Consequently, what is "one" referring to in the following sentence: "Furthermore, we noted that the mean for every non-confining region is approximately one, …"

Reply: Thank you for your careful observation. In Figure 3 b and c the data are normalized to the mean of the nuclear area and the mean of the relative highly-condensed area, respectively, when the nucleus is unconfined, i.e. mean among every frame in which the nucleus lies within a non-confining region (Entry, N1, N2…).

We firstly considered normalizing with the mean of the variable at the entry of the channel; however, some cells started the analysis further downstream the channel. Most of the time these cells were already migrating when the time-lapse experiment started or there were more than one cell at the Entry and, hence, those frames could not be considered for the analysis. In addition, when cells first enter the microchannel, they deform from a 3D spherical shape into a vertically confined disc-like morphology, which increased the variability of the data at the Entry. Consequently, normalizing the data to the average value of the non-confined nucleus proved to be more reliable and widely applicable. Note that the single-cell analysis showed that nuclear area exhibited a growing trend and that chromatin condensation levels were consistently recovered after confinement. Nuclear growth implies that the area at the Entry is smaller than the mean nuclear area among all non-confinements (corresponding to 1 in Figure 3b), then, normalized nuclear area at the Entry is lower than 1. On the other hand, reversible chromatin condensation means that the normalized condensation value at the Entry and at every other non-confining region (N1, N2, …) are similar, hence, they are centered around 1.

We agree that our explanation in the manuscript might not be sufficiently clear, and we included the following statements in Results section 2.4:

"Each point in a column group corresponds to an individual cell, and it represents the average of the measured variable among every frame in which the geometric center of the cell lies within the specified region. Note that this data point is normalized with the mean of the variable among all non-confining regions (Entry, N1, N2…).

…

Furthermore, we noted that the mean for every non-confining region is approximately one, i.e. a cell has a similar condensed area in every non-confining region (p-values between non-confining regions failed to meet the significance criterion, see Supplementary Spreadsheet S1). This supports the idea of a basal chromatin condensation level; nuclei stably recover their original condensation level after every constriction, proving the reversibility of global chromatin condensation in these confinement devices."

13. In Figure 4B, annotate Acon and Atot in the legend.

Reply: Thank you for your comment. To improve clarity and standardize the labeling throughout the manuscript, we decided to replace A_{con} and A_{tot} with $A_{cluster}$ and $A_{nucleus}$, respectively. Additionally, a description for these labels has been included in the caption for Figure 4.

14. The description on H3K27me3 and H3K9me3 from the Method section should be included in the Results section. This will provide context to the reader on why these markers are chosen to begin with.

Reply: Thank you for helpful suggestion, the description of the heterochromatin markers has also been included in the Results section 2.6:

"Therefore, we performed an immunofluorescent experiment using two well-established heterochromatin markers H3K27me^3 (cyan) and H3K9me^3 (magenta), which target two different chemical modifications on histone H3. Trimethylation of lysine 9 on histone H3 (H3K9me^3) is associated with constitutive heterochromatin, which is mostly located in centromeric and telomeric DNA regions, while trimethylation of lysine 27 on histone H3 (H3K27me^3) is associated with facultative heterochromatin, which is developmentally regulated.

Mapping these markers together with the GFP channel (green), to capture intrinsic GFP expression from the chromatin labeling on H2B, we could visualize the distribution of heterochromatin in chromatin content."

15. "It is noteworthy that H3K9me3 marker (magenta channel) is preferentially expressed in the nuclear periphery and around the nucleolus (Figure 5) …" – Isn't the H3K27me3 also enriched at the nuclear periphery and around the nucleolus?

Reply: We appreciate your careful observation. Although the H3K27me3 marker can be found near the nuclear periphery and nucleolus, these are not its preferred locations; unlike H3K9me3, H3K27me3 loci are frequently and evenly distributed throughout the nuclear interior (see the segmentation in Figure 5c,f). This distribution explains why the correlation coefficient between H2B-GFP and the H3K27me3 marker is significantly higher than that observed for H3K9me3. Interestingly, the accumulation of the H3K27me3 marker at the nuclear periphery becomes more pronounced during confinement.

16. In Figure 5, H3K9me3 and H3K27me3 are immunostained, not GFP fusions; the "GFP" label should be removed.

Reply: Thank you for noting this. The "GFP" label was removed accordingly.

17. Figure 5B should be presented later in the figure, as it is the conclusive data from the images.

Reply: We agree with your comment; however, due to the distribution of the panels, the correlation coefficient graph could only fit in that upper right corner.

18. "The recovery is not complete, since the peak in chromatin density shifts to smaller values compared to nuclei before the confinement (Figure 6c)." – this is not clear, which part of the data show this observation?

Reply: We thank the reviewer for pointing this out. The text references the wrong figure, the label should be Figure 6e, where the density distributions are represented. Additionally, in response to the reviewer's next comment, we have clearly indicated the positions of the peaks in Figure 6e, hoping to provide a clearer explanation.

19. Figure 6E is very hard to follow. The text refers the figure in seconds while the data is in minutes. Please consider changing the color scheme as it is very hard to distinguish the early time points. Arrows with different colors (with description in the figure legend) might help in describing the statement in the text: "The widening in chromatin distribution during confinement is appreciated by comparing the histograms for t = 270 s and t = 541 s. The height of the peak decreases, and the tail of the distribution rises. After confinement, corresponding to t = 1081 s and t = 1622 s, density distribution is partially recovered (ρ = 0.2). The values of the density distribution for ρ > 0.2 are higher than for the unconstricted nucleus, suggesting a certain degree of irreversible behavior after confinement."

Reply: We agree with the reviewer's comments. Following these suggestions, the units in Figure 6 have been set to minutes and we have modified Figure 6e to indicate the position of the peak of each distribution curve, hoping to improve clarity. The section of the Supplementary Material below has been rewritten:

"The widening in chromatin distribution during confinement is appreciated by comparing the histograms for t = 5 min and t = 9 min. The height of the peak decreases, and the tail of the distribution rises. After confinement, corresponding to t = 18 min and t = 28 min, the density distribution is partially recovered (ρ = 0.2). The values of the density distribution for ρ > 0.2 are higher than for the unconstricted nucleus, suggesting a certain degree of irreversible behavior after confinement."

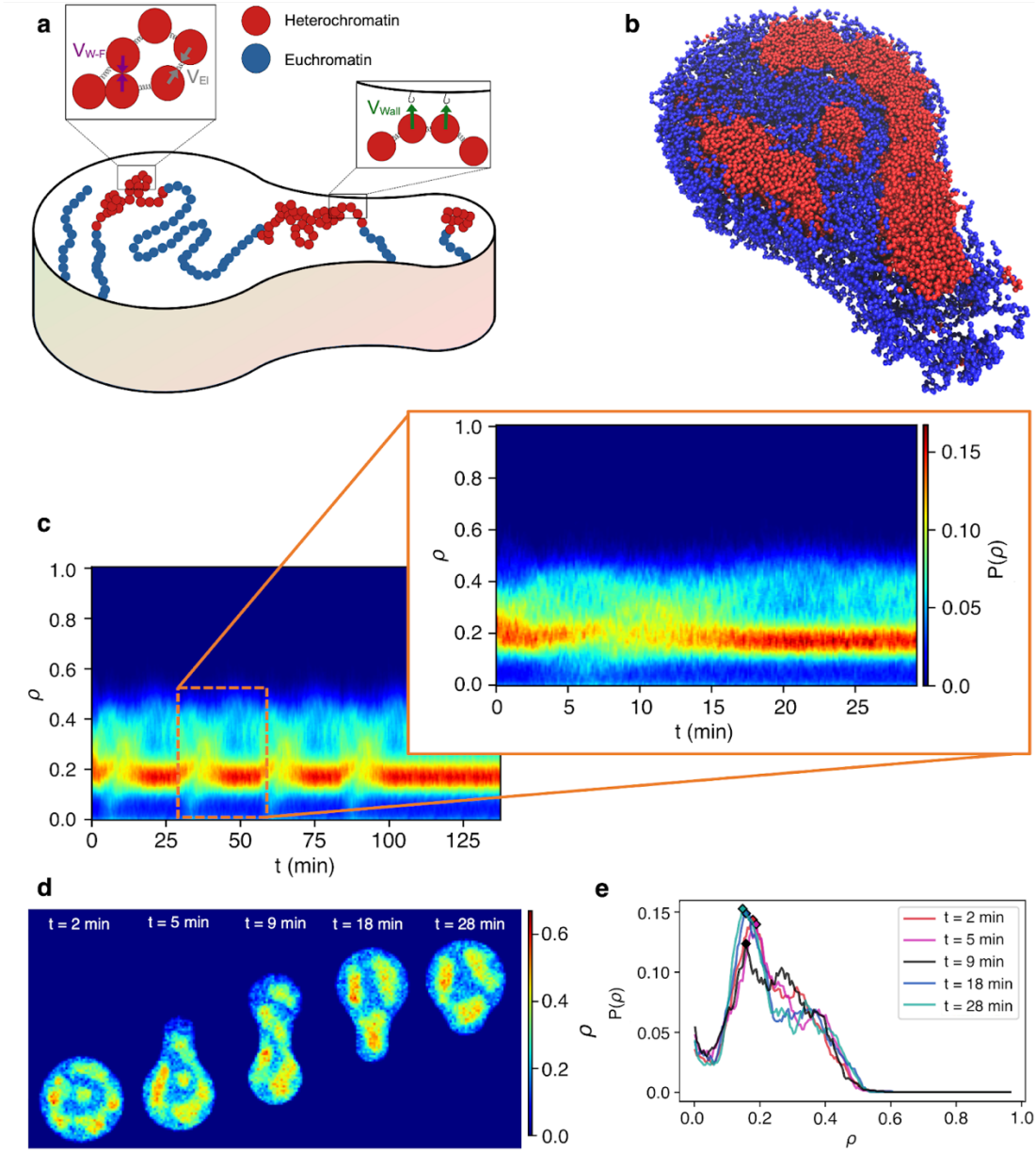

Fig. 6. Polymer model to simulate chromatin dynamics during cell migration through a confinement. a. Schematic of the chromatin model showing heterochromatin (in red), euchromatin (in blue) and elastic (V_{el}), Wang-Frenkel ($V_{W\text{-}F}$) and Wall (V_{Wall}) potentials in the insets of the figure. The geometry corresponds to a cell nucleus traversing a constriction within the microchannel. **b.** Three-dimensional polymer representation of chromatin (heterochromatin beads in red and euchromatin beads in blue) within the nucleus as it enters a constriction (t = 5 min). The figure shows the bottom region of the nucleus, sectioned at the mid-width plane. **c.** Colormap depicting the evolution over time (horizontal axis) of the histogram of chromatin density (vertical axis) for a chromatin chain of N=60000 and average domain size of 64 beads. The colormap corresponds to the pixel proportion with a particular density. The zoomed-in graph (right) represents chromatin density profile for the simulation performed (30 minutes long) while the complete graph (left) displays a repetition of the simulation result (i.e. the zoomed-in graph) to reproduce the experimental time-scale for successive confinements in fast migrating cells. **d.** Chromatin density distribution within the nucleus as it dynamically deforms to replicate the migration through a constriction in the microchannel. The time corresponding to each snapshot is shown on the top. **e.** Histograms for chromatin density at different time points of the simulation, each corresponding to a column in the zoomed-in graph in panel c. The diamond symbols indicate the maximum of each distribution.

20. "We find that the distribution for small chromatin cluster sizes is not characterized by a power-law distribution as in the case of nucleoli [43, 44] but by an exponential distribution, similar to that observed for intracellular protein condensates [42]." – please provide more explanation on this statement.

Reply: Thank you for highlighting this issue. We have modified the statement to relate the distributions directly with the observed trend in our results (Figure 4):

"We find that the distribution for small chromatin cluster sizes is not characterized by a power-law distribution as in the case of nucleoli [46, 47] but by an exponential distribution (a linear decay at the beginning of our histograms in logarithmic scale), similar to that observed for intracellular protein condensates [45]."

21. "However, we consistently find probability peaks at higher cluster areas during confinement, which are absent in the case of protein condensates or nuclear speckles [42]." – what "probability peaks at higher cluster areas" means, how it correlate with Reference [42], and what is the impact of this comparison?

Reply: Thank you for raising this concern. Note that the histograms in Figure 4 are normalized with the total number of counts, therefore, the vertical axis represents the probability of finding the cluster sizes in the horizontal axis. The study by Lee et al. [45] describes an exponential distribution for the size of protein condensates as an intracellular organization strategy. In our case, we found a similar exponential distribution (corresponding to a linear decay in our logarithmic scale). Nevertheless, this exponential distribution is only true for small cluster sizes at the beginning of the histograms. For large clusters we no longer observe the linear decay but an increase in the normalized bin count, hence, a peak in the probability of finding larger clusters, particularly during confinement. This comparison shows how different distributions have been proposed to describe the sizes of cellular condensates and provides a possible explanation for the formation of small chromatin clusters: this distribution can be associated to a quench-then-coalesce mechanism [45].

To improve clarity, we modified the statement in the Discussion:

"However, we consistently find probability peaks at higher cluster areas during confinement, which are absent in the case of protein condensates or nuclear speckles [45]. These peaks at larger cluster areas imply a growth of chromatin clusters upon deformation."

And we added the statement below in the Results section 2.5:

"Therefore, each column in the histogram represents the normalized number of clusters of a relative area that appear among all nuclei and all time steps in the experiments for a specific region. Note that the histograms are normalized with the total number of counts, therefore, the vertical axis represents the probability for the cluster sizes in the horizontal axis."

22. Product codes for antibodies are missing and should be provided.

Reply: Thank you for pointing this out. We included the product codes for the antibodies in the Methods section 4.7:

"Subsequently, we incubated the microfluidic device overnight with the two primary antibodies specific against different heterochromatin markers: Anti-Histone H3 (tri methyl K9) antibody (ab8898, Abcam) and Anti-Histone H3 (tri methyl K27) antibody (ab6002, Abcam)."